2008-01-01

Analysis of the Generation of Auditory Steady-State Cortical Evoked Responses in Guinea Pigs

Jose Alejandro Briceno
University of Miami, jbriceno511x@gmail.com

UNIVERSITY OF MIAMI

ANALYSIS OF THE GENERATION OF AUDITORY STEADY-STATE CORTICAL EVOKED RESPONSES IN GUINEA PIGS

By

José Alejandro Briceño

A THESIS

Submitted to the Faculty
of the University of Miami
in partial fulfillment of the requirements for
the degree of Master of Science

Coral Gables, Florida

August 2008

UNIVERSITY OF MIAMI

A thesis submitted in partial fulfillment of
the requirements for the degree of
Master of Science

ANALYSIS OF THE GENERATION OF AUDITORY STEADY-STATE CORTICAL EVOKED RESPONSES IN GUINEA PIGS

José Alejandro Briceño

Approved:

_____	_____
Özcan Özdamar, Ph.D.	Terri A. Scandura, Ph.D.
Professor of Biomedical Engineering	Dean of the Graduate School
_____	_____
Jorge Bohórquez, Ph.D.	Richard McNeer, M.D., Ph.D.
Research Assistant Professor	Assistant Professor
of Biomedical Engineering	of Anesthesiology

BRICEÑO, JOSÉ ALEJANDRO (M.S., Biomedical Engineering)
Analysis of the Generation of Auditory Steady-State Cortical Evoked Responses in Guinea Pigs (August 2008)

Abstract of a thesis at the University of Miami.

Thesis supervised by Professor Özcan Özdamar.
No. of pages in text. (76)

Recent research shows that human auditory steady-state responses (ASSRs) develop a resonance at 40 Hz and the dramatic amplitude increase of the P_b component of the middle latency response (MLR) accounts for the high amplitude of the ASSR at 40 Hz. The first part of this study aimed to investigate the ASSR resonance characteristics as a function of rate in guinea pigs. A study of the grand average of the peak-to-peak and fundamental frequency amplitudes does indeed show a resonance around 40 Hz in guinea pigs. Unlike human ASSRs, this resonance is very broad (26-52 Hz) and flat. The centrally recorded ASSRs are smaller and tend to have resonances at higher rates compared to temporal signals.

The second part of the analysis investigated whether the superposition of transient responses can predict the acquired ASSRs at each corresponding rate. This superposition theory is one of two competing theories on the origin of the ASSRs, with the other centering on the induced phase synchronization of brain waves. In order to test the first theory, transient responses were used to create synthetic ASSRs, which were then compared to the acquired ASSRs via correlation coefficient and phasor analysis. For the 40 Hz ASSR, both temporal and central electrode synthesized ASSRs show a correlation coefficient above 0.80. In the comparison at 20 Hz, the correlation coefficient is very

high (~0.9) in the temporal electrode, yet significantly lower (~0.7) for the central electrode. Furthermore, at 80 Hz, the correlation coefficient is significantly lower in both temporal and central electrodes (~0.7). At all rates, the correlation coefficients are highest with low jitter sequences.

Finally, phasor analysis was also used to test the superposition theory of the generation of the acquired ASSRs at 20, 40, and 80 Hz. Overall, in the temporal recordings at 40 Hz, the superposition of the MLR responses accurately predicted the acquired 40 Hz ASSR as demonstrated by both magnitude and phase analysis. The recordings made in the central electrode only predicted the acquired ASSR in its phases, with significant differences found in magnitude at its main harmonics. Similarly, at 20 and 80 Hz in both temporal and central electrodes, the synthetic ASSRs did not appear to fully predict the acquired ASSRs. Although the phases were successfully predicted, large magnitude variations were observed. As shown by mean prediction error plots, the acquired ASSRs are best predicted by low jitter sequences, followed by low-medium and medium jitter sequences.

DEDICATION

This research is dedicated to my family.

They have always believed in me and supported every endeavor I have ever pursued.

I would also like to thank God for blessing me with the opportunity to pursue higher education and providing me with the resources I needed along the way.

"I can do everything through him who gives me strength."

- Philippians 4:13

ACKNOWLEDGEMENTS

I would like to thank my mentor Dr. Özcan Özdamar for providing me with all the tools I've needed along the way. Overall, Dr. Özdamar did an excellent job in guiding me in the right direction as I presented him with the various results I obtained from my research. I've also noticed that he deeply cares for all of his students by always working with them side by side.

One of the toughest challenges I faced was learning to efficiently program using Matlab in order to analyze the recorded data. I would like to thank Dr. Jorge Bohórquez for guiding me through this process. He also provided me with various sample programs for me to study in order to use proper programming techniques.

Throughout the spring semester of 2008, I had the pleasure of working with two visiting Turkish professors, Dr. Serdar Demirtas and Dr. Suha Yagcioglu. Dr. Demirtas greatly contributed to my research in various ways. First, he performed the surgeries on all the guinea pigs that were part of this study. In addition, he also contributed many afternoons helping me organize the large amount of data. I would like to thank Dr. Yagcioglu for teaching me various programming techniques and helping in the analysis of my data.

I would also like to thank Dr. Thomas R. Van De Water from University of Miami Ear Institute for funding my project. Finally, I would like to thank the other Neurosensory graduate students for reviewing many signal processing fundamentals which I could have overlooked during the analysis of the data.

TABLE OF CONTENTS

Page

LIST OF FIGURES

LIST OF TABLES

CHAPTER 1: INTRODUCTION AND OBJECTIVES

A myriad of brain responses, including auditory function, can be evaluated objectively by electroencephalography (EEG), which works by recording the bioelectric activity produced by the brain. More precisely, it is a measure of the extracellular current flow associated with the summation of many neurons. In the presence of auditory stimuli, these patterns undergo specific repeatable changes. Using stimulus triggered averaging, a signal processing technique, the background EEG data is greatly reduced, resulting in the waveform known as an auditory evoked response (AER). AERs can be classified as a transient response or steady-state response (ASSR), depending on the applied stimulus. A low rate stimulus without overlapping responses generates a transient response. On the other hand, isochronic stimuli with overlapping responses generate an ASSR, with a response characterized by its periodic nature.

The AERs consist of several peaks and troughs which represent the synchronous activation of different portions of the auditory pathways, which makes it a useful tool in determining the integrity of the auditory system. More specifically, high sensitivity of AERs can help physicians detect and localize lesions in a noninvasive manner. In a similar fashion, vision and touch can also be measured using visual evoked responses (VERs) and somatosensory evoked responses (SERs).

The objective of this study is to investigate how the transient and steady-state responses (ASSRs) from awake-restrained guinea pigs at varying stimulation rates relate to each other and whether the ASSRs can be predicted from the transient responses.

The main research question is to investigate the relationships and distinctions of the human and mammal auditory responses. It involves the investigation of a possible

resonance and an attempt to predict the acquired ASSRs through the convolution of its respective transient responses. Another research objective is to investigate any further phenomena which could reveal further insights into the inner workings of a guinea pig brain's auditory pathway. This investigation is significant since it could contribute to the understanding of ASSRs and the source of their generation.

In order to meet the objectives, several signal processing techniques, including: cross correlation, convolution and deconvolution, fast fourier transform, inverse fast fourier transform, and phasor analysis are utilized using MatLab.

In summary, this research project will investigate the resonance characteristics of ASSRs as a function of rate, test the validity of the superposition theory for the generation of ASSRs through its synthetic generation, and search for other possible phenomena in the acquired ASSRs.

CHAPTER 2: BACKGROUND

2.1 Auditory Evoked Responses (AERs) in Humans

The electroencephalogram (EEG) is a test that measures the bioelectric activity produced by the brain. This activity is the result of the conglomeration of sensory, motor, cognitive and behavioral factors, generating electrical activity. In the presence of an auditory stimulus supplied through the headphones, these patterns include the presence of auditory evoked responses (AERs). Since AERs are embedded in the EEG waves, they can be extracted by the averaging of the collected signals. This simple technique also helps to minimize the effects of ambient noise.

AERs can take the form of a transient response or auditory steady-state response (ASSR), depending on the applied stimulus. **Figure 2.1** shows how to obtain a transient response with constant rate (non-overlapping) stimuli. As discussed earlier, averaging is then utilized to obtain the transient response. **Figure 2.2** shows another method of obtaining a transient response, which allows for much higher acquisition rates using jittered stimuli at specific predetermined points. The averaged response generated, the quasi ASSR, resembles an acquired ASSR, but it is actually the result of an overlap of the transient responses. The quasi ASSR can then be separated into its individual transient responses using the CLAD algorithm. This method has the advantage of having much higher acquisition rates, which reduces total recording time and minimizes the recording of fluctuating MLRs due to changes in a subject's state.

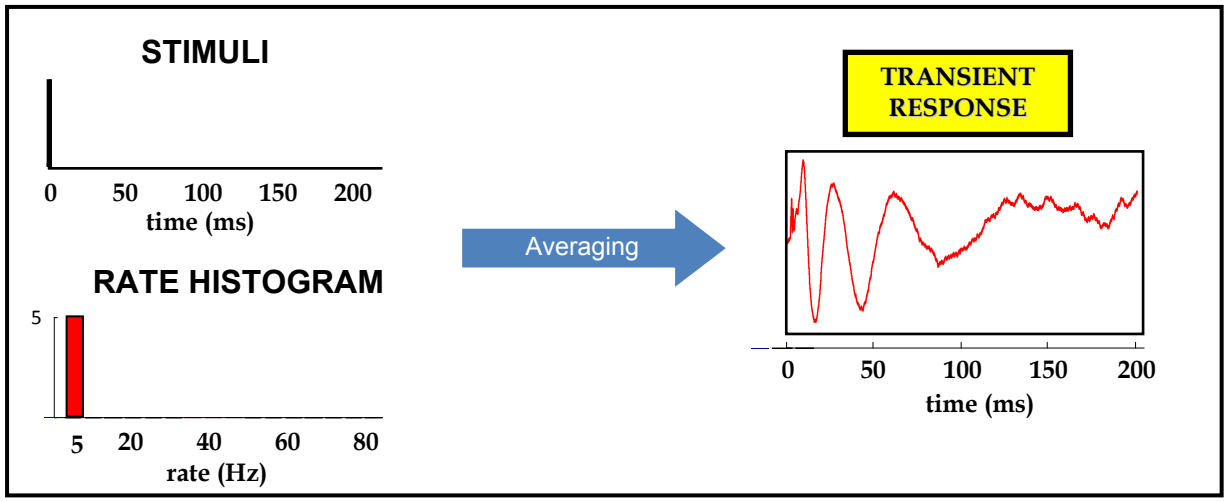

Figure 2.1. Steps for obtaining a transient response with standard stimuli (constant rate: 5Hz).

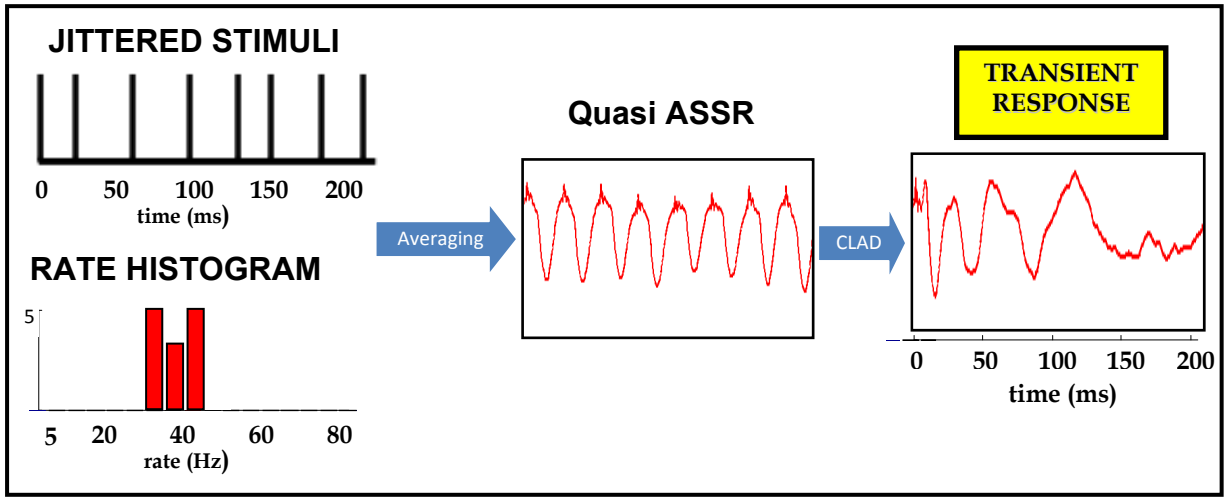

Figure 2.2. Steps for obtaining a transient response with jittered stimuli (40Hz).

Figure 2.3 shows the procedure for obtaining the acquired ASSRs. In this example, clicks are applied at a frequency of 40 Hz and spaced equally, which generates an averaged response characterized by its periodic shape. This steady-state property is analogous to the adaptation effects that occur in the other senses, including vision and touch.

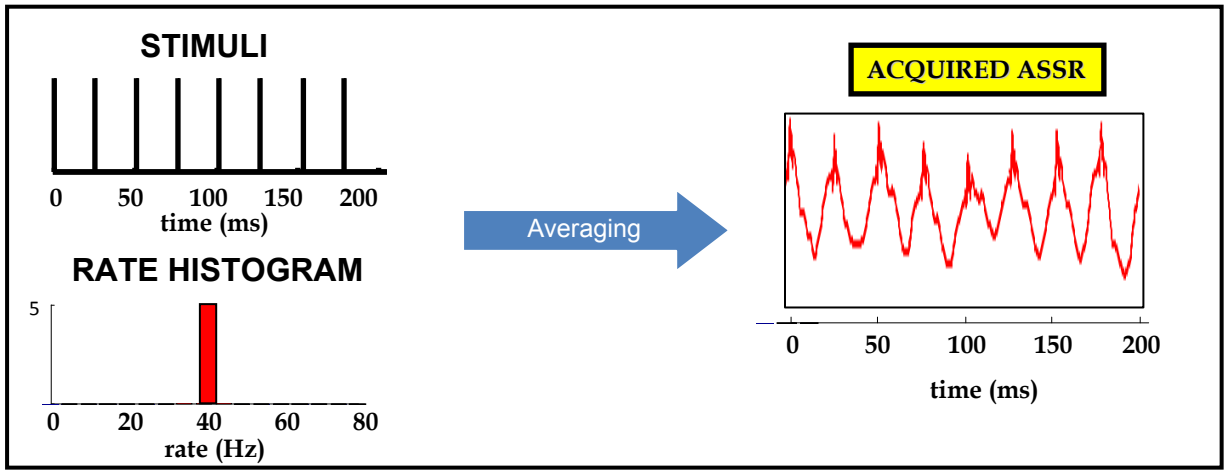

Figure 2.3. Steps for obtaining acquired 40 Hz ASSRs

2.1.1 Transient Response

A transient response is usually described in terms of peak amplitudes and latencies in the time domain. In clinical practice, the response can be divided into the auditory brainstem response (ABR), middle latency response (MLR) and late latency response (LLR) components, each corresponding to a time segment of the total response. **Figure 2.4** shows the three main classifications along with its respective peak amplitudes. Since the source of each of these time segments corresponds to a specific origin in the brain, their analysis is utilized to diagnose various neurological conditions noninvasively.

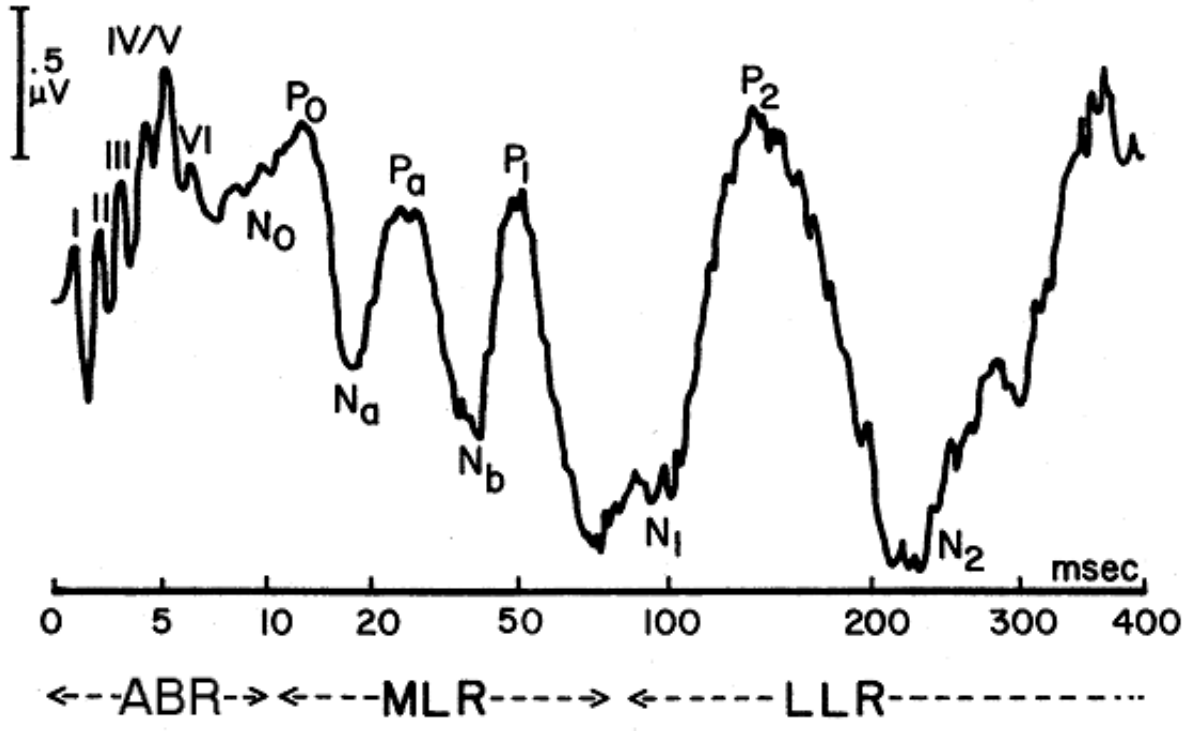

Figure 2.4. AER classification in humans (modified from Michelini et al., 1982).

The ABRs, composed of five to seven positive peaks that occur between 2-15 ms, have been shown to be generated by the activation of the primary auditory pathways from the auditory nerve to the inferior colliculus. For a click stimulus presented at 10 Hz and

60 dB above normal hearing threshold, Wave I occurs at about 1.7 ms, Wave II at about 2.8 ms, Wave III at about 3.9 ms, Wave IV at about 5.1 ms, Wave V at about 5.7 ms, and Wave VI at about 7.3 ms (Hood & Berlin, 1986; Chiappa, 1990). The ABR is believed to be independent of the state of the patient and can therefore be obtained in aware or sleep states. Its clinical applications include: detection of hearing disorders, determining the presence of tumors and lesions along the VIII nerve, screening for retrocochlear pathology, and detection of various neurological diseases.

The MLRs, with a latency range between 15-80 ms, originates in the thalamus and primary auditory cortex (Kraus et al., 1982; Özdamar et al., 1982, Özdamar & Kraus, 1983). It is composed of various vertex negative and positive peaks, including: N_a, P_a, and P_b, occurring at approximately 18, 30, and 50 ms, respectively. Since its origin involves the thalamo-cortical pathway and reticular formation, it has been found to be affected by the arousal of a subject. In fact, recordings under anesthesia and various stages of sleep display a shift in the latencies and amplitude decrease in the MLR waves. Thus, MLR recordings can be a useful intraoperative tool when monitoring cortical function of depth of anesthesia during surgery. Other MLR's clinical applications include: assessment of cochlear implant function, localizing auditory pathway lesions, and determining hearing thresholds.

Finally, the LLR's latency range is 80-250 ms and originates in the temporal and adjacent parietal areas. It is characterized by low frequency waves of around 4-5 Hz and large amplitudes, ranging between 3 to 10 microvolts. The peaks represent the expected voltage polarity of the response. As a result of a click stimulus, the peaks include: N1, P2, N2, P300, occurring at approximately 100-150, 150-200, 180-250, and 300 ms,

respectively. Since LLR waves vary with the subject's age, sleep stage, and state of arousal, its analysis proves to be a useful tool only in subjects that are alert and cooperative during testing. Clinical applications include: determining cognitive ability as a result of head injuries (Greenberg et al, 1981), analyzing the effects of aging and Alzheimer's, and detecting Multiple Sclerosis (Robinson & Rudge, 1977). In addition, it can be used to diagnose various cognitive and psychiatric disorders.

2.1.2 Auditory Steady-State Response

An auditory steady-state response (ASSR) is generated by presenting the ear with an isochronic stimulus that produces overlapping responses. This response eventually takes the form of a periodic signal with frequency components that remain constant in amplitude and phase over time, as shown in **Figure 2.5** (Regan, 1989). As opposed to transient responses, which are evoked by stimuli that allow the response of one stimulus to die off before the next one, an ASSR is evoked by stimuli with shorter inter-stimulus intervals. Utilizing this shorter interval allows the transient response to any one stimulus to overlap with the response to a succeeding stimulus (Lins et al., 1995).

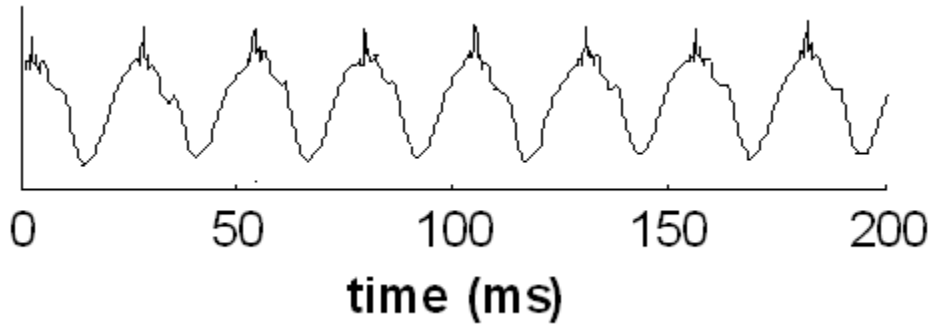

Figure 2.5 A typical guinea pig 40Hz ASSR (Session # 13)

ASSRs have been thought to be generated by the superposition of the components of the MLRs (Galambos et al., 1981) or due to a 40 Hz resonance triggered by auditory stimuli (Basar et al., 1987). Recent human studies (Özdamar & Bohórquez, 2007) have shown that a P_b resonance of the MLR at around 40 Hz explains the rate characteristics of the ASSR.

Unlike transient responses, which are described in terms of amplitudes and latencies, an ASSR is usually described in its frequency domain. Using Fourier transformation, the ASSR wave is broken down into an amplitude and phase component that can be displayed in a polar plot. The resulting plot contains a vector extending outwards from its origin. The length of the vector corresponds to the magnitude, while the angle between the vector and the x-axis measured counter-clockwise provides the phase information.

Ensuring an isochronic stimuli, various waveforms can be used to envoke an ASSR, including: sinusoidal amplitude modulation (SAM), frequency modulation (FM), mixed modulation (MM), independent amplitude and frequency modulation (IAFM), tones, and beats (**Figure 2.6**). In fact, ASSRs can be classified into three mains types according to the stimulus utilized during recording. First, the utilization of continuous tones generate frequency following responses (FFR). Second, a repeating individual, non-continuous stimuli yields a discrete stimuli evoked ASSR. Third, modulating carrier frequencies, such as amplitude modulation (AM) and frequency modulation (FM), generates modulated continous stimuli evoked ASSRs.

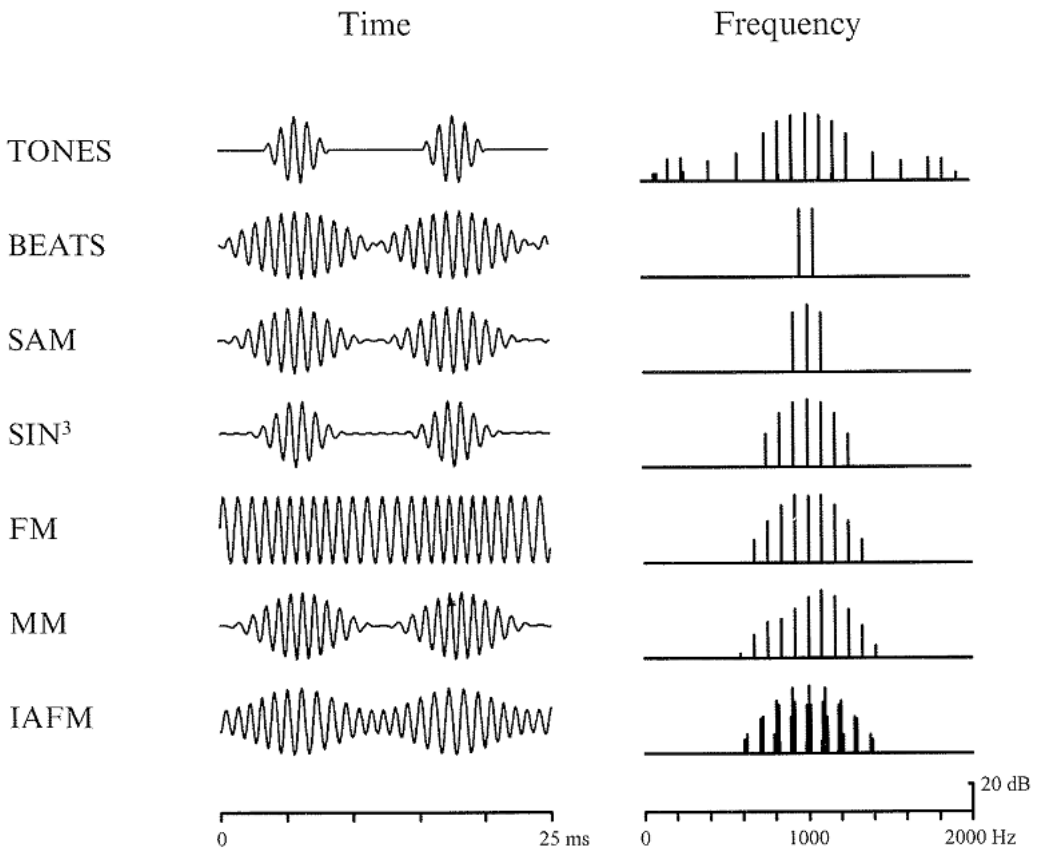

Figure 2.6. Stimuli used to evoke ASSRs. The stimulus waveforms are plotted in time domain on the left, and the spectra of the stimuli are shown on the right. These data were obtained by calculation; electric and acoustic waveforms would be basically similar, with some filtering effects during passage through the signal generators and transducers. Tones represent brief tone-bursts of 1000 Hz with the commonly used 2-1-2 envelope, with rise and fall times of two cycles (2 ms) and a plateau of 1 cycle (1 ms). The beats were obtained by adding together continuous tones of 958 and 1042 Hz. SAM tone used a carrier of 1000 Hz and a modulation frequency of 84 Hz. The SIN^3 tone used a modulation envelope base on the third power of the usual sinusoidal envelope. The FM tone is sinusoidally modulated with a depth of modulation of 25%. The MM tone has mixed modulation (100% AM and 25% FM), with both modulations occurring at 84 Hz. The bottom set of data represent independent amplitude and frequency modulation (IAFM), with 50 % amplitude modulation at 84 Hz and 25% frequency modulation at 98 Hz. All the time waveforms are plotted so that they have the same peak amplitudes. The spectra are plotted logarithmically over a range of 50 dB relative to the maximum peak in the spectrum (Picton et al., 2003).

2.1.2.1 40 Hz Response

Since the presentation of discrete stimuli results in the overalapping of the responses, certain frequencies have been found to produce a resonance due to the underlying waveforms' timing and frequency characteristics. In particular, the 40 Hz and

80 Hz responses have generated an enhancement as compared to other frequencies. After the 40 Hz ASSR was first studied by Galambos et al. (1981), the great majority of ASSR research has focused on the stimulation rates at 40 Hz and 80 Hz. In this study, Galambos and his colleagues demonstrated that when a stimulus is presented at 40 Hz, the MLRs have an amplitude about 2 or 3 times greater than when the stimulus is presented at a rate of 10 Hz. At the time, they concluded that the resonance at 40 Hz was a result of the superpositioning of the successive peaks. In addition, they noticed that the 40 Hz resonance was reduced due to drowsiness, sleep, and anesthesia. The particular effect from anesthesia made it a potentially useful tool in monitoring patients under sedation (Galambos et al., 1981; Stapells et al., 1984; Plourde & Picton, 1990; Hori et al., 1993). In fact, after these effects were shown to occur in the other sensory systems, it was proposed that a gamma range (30-50 Hz) brain activity is required for adequate awareness of the sensory information (Galambos, 1982; Galambos & Makeig, 1988; Basar et al., 1987; Bressler, 1990; Patterson et al., 1998).

2.1.2.2 80 Hz Response

One of the drawbacks to the 40 Hz response is its unreliability in young infants, which is believed to be as a result of the early development state of the auditory cortex and its immature connections (Stapells et al., 1988; Levi et al., 1993; Linden et al., 1985). In addition, although its effects on anesthesia are often appreciated, some clinical applications consider it a disadvantage that the resonance is affected by sleep and anesthesia. In order to circumvent these disadvantages, numerous studies looked for other high amplitude ASSRs that could provide the same benefits. Several researchers

found that the 80 Hz response, which represents the 70-110 Hz region, was not affected by sleep, anesthesia, and even during recordings in young children and newborns. In fact, it is now used for the testing of the human auditory physiology and in the administration of objective audiometry in both adults and young children (Cohen et al., 1991; Levi et al., 1993; Lins et al., 1995; Aoyagi et al., 1993; Rickards et al., 1994; Lins et al., 1996).

2.2 Auditory Evoked Responses (AERs) in Animals

2.2.1 Transient Response

AERs in guinea pigs and other animals show both similar and different characteristics to those in humans. Depending on the stimuli, they can take the form of a transient response or auditory steady-state response (ASSR). **Figure 2.7** shows the transient ABR and MLR for the guinea pig, cat, and humans. As in humans, these waves can be divided into three sequential parts: auditory brain-stem response (ABR), middle latency response (MLR), and long latency response (LLR). The latencies for each portion vary amongst mammals.

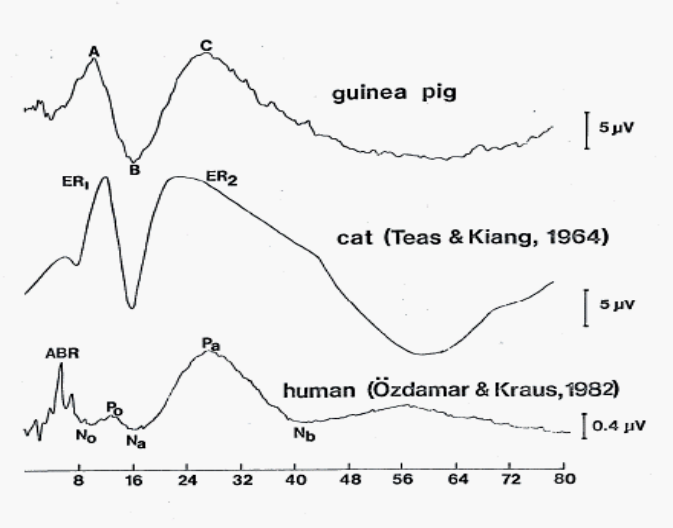

Figure 2.7. Auditory Evoked Response of various mammals (McGee et al., 1983).

As shown above, the MLR response of the cat and guinea pig show very similar results. Monaural stimulation in an unanesthetized cat produces a response characterized by two positive peaks at around 12-14 ms and 22-29 ms, and two negative troughs at around 17 ms and 45-73 ms (Kiang et al., 1961; Teas et al., 1964; Mäkelä et al., 1990). Similarily, in unanesthetized guinea pigs, the contralateral

(temporal) response shows a positive peak at a latency of approximately 12 ms and 27 ms, and a negative trough at 17 ms (McGee et al., 1983). In both guinea pigs (McGee et al., 1983; Goksoy & Utkucal, 2000) and cats (Buchwald et al., 1981), the MLRs have been shown to be greatly altered by anesthesia, including reduction in amplitudes and more prolonged latency times. Overall, in comparison to cats, guinea pigs are advantageous experimental animals since they are less expensive and easier to handle.

In guinea pigs and cats, the largest amplitude response is generated over the hemisphere contralateral (temporal) to the stimulated ear, while the human MLR component P_a is largest at the vertex, suggesting symmetry over the temporal lobes (Özdamar & Kraus, 1983; Özdamar, et al., 1982). Thus, according to McGee, et al. (1983), there appears to be a bilateral generation of the MLR in the human but unilateral generation in the guinea pig. The guinea pig and human responses also show some differences in waveforms and absolute latencies. These major distinctions between the MLRs have resulted in a different naming convention for the MLR peaks in guinea pigs and other animals.

In a study by McGee et al. (1983), the latencies of both guinea pig and human MLRs were found to be generally stable, with only slight increases, as a result of stimulus intensity. In addition, the amplitude-intensity function for the major waves of the guinea pig was found to be similar in shape to the function for the human P_a. The amplitude of both displayed large standard deviations, indicating a large variability. The effects of stimulus rate in guinea pigs resulted in amplitude increases as repetition rate decreased. At lower frequencies, the effects of anesthesia resulted

in greatly altered waveform structure and prolonged peak frequencies. At higher frequencies, anesthesia resulted in the elimination of several of the MLR peaks.

Recently, a study by Demirtas and Özdamar (2008), has shown in guinea pigs that the ampalitude of wave A, B, and C of the MLRs decrease gradually as the rate increases. In particular, a resonance of wave C was observed to increase in the recordings with 39.1 Hz. These results are significant since it parallels the human study (Özdamar & Bohórquez, 2007), which demonstrates that there is a P_b resonance of the MLR at around 40Hz which explains the rate characteristizes of the 40 Hz ASSR. One of the analysis in the current study presentated will explore a resonance near 40 Hz ASSRs, which could link to the recently discovered wave C resonance near 40 Hz.

Figure 2.8 shows the AEPs from various electrode placements in the guinea pigs. For this particular project, the temporal lobe is the most important since it provides the MLR waves with the largest amplitudes. On the other hand, ABR waves showed the largest responses on the occipital lobe and ipsilateral side close to the stimulation ear. As discussed in the methods section, this project used electrode placements in the central and temporal regions of the guinea pig brain.

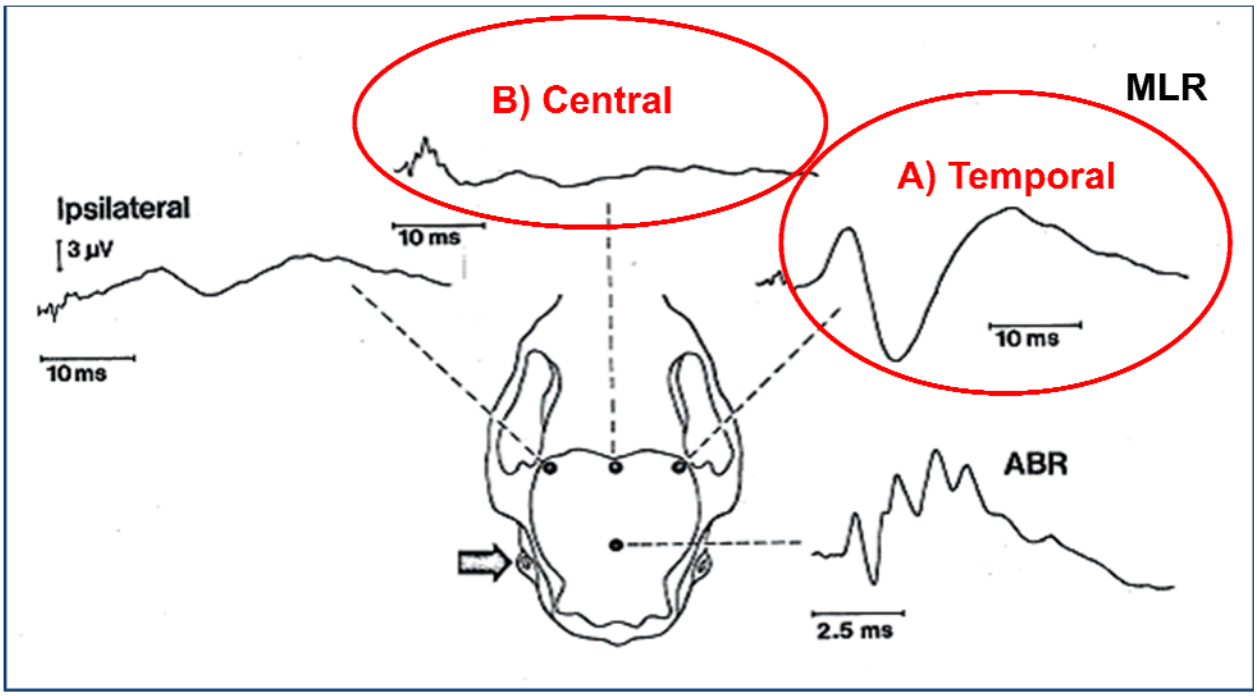

Figure 2.8. Sample recordings from four electrode locations in guinea pigs (McGee et al., 1983).

2.2.2 Auditory Steady-State Response

An auditory steady-state response (ASSR) is generated by presenting the ear with fast repetitive stimuli, such that a constant amplitude and phase response is generated, characterized with a periodic shape. Animals ASSRs have been studied in cats (Mäkelä et al., 1990), rabbits (Ottovani, et al., 1990), and rats (Conti et al., 1999).

In a study of six cats (Mäkelä et al., 1990), the ASSRs from the auditory cortices were studied in response to 350 ms trains of clicks with 10-100 Hz repetition rate. The ASSRs were found to be small or absent below 30 Hz and in the 60-70 Hz range. Overall, a clear increase in the averaged Fourier amplitude values were observed at stimulation frequencies of 25-40 Hz, with the maximum at 30 Hz. Similarly, in rabbits (Ottovani, et al., 1990), the best repetition rate is around 30 Hz, while in rats

(Conti et al., 1999), it appears to be 50 Hz. Furthermore, in both guinea pigs (Yoshida et al., 1984) and humans (Galambos et al., 1981; Stapells et al., 1984), the optimal frequency has been observed at 40 Hz. Mäkelä et. al (1990) argues that species differences in the latencies of the main peaks of the MLRs explains the differences in ASSR resonances since it generates differences in the resulting superposition of the waves. In addition, the authors state that different recording techniques and more complex interactions within cortical structures may underlie the generation of the ASSR.

The ASSRs in the cat study (Mäkelä et al., 1990) were also recorded from the medial geniculate body (midbrain), vertex, visual and associate cortices, and from the hippocampus. ASSRs recorded from the median geniculate body were found to be more resistant to barbiturate anesthesia, where the cortical ASSRs were greatly suppressed. Similarly, in a study on guinea pigs by Yoshida et al. (1984), the authors suggest that the ASSRs originate from both the auditory cortex and midbrain. As in the cats, the cortical ASSRs were very sensitive to barbiturate anesthesia, while the midbrain ASSRs were not. According to Mäkelä et al. (1990), among the auditory cortex and MGB, the auditory ASSRs in a human resembles most the ASSRs from the cat auditory cortex. However, human ASSRs could also contain subcortical contributions (Galambos, 1982; Firsching et al., 1987; Spydell et al., 1985).

In cats, ASSRs recorded from the vertex, visual cortices, and hippocampus show low amplitude or no ASSRs (Mäkelä et al., 1990). This is probably due to different orientations of the cat and human auditory cortices with respect to the vertex. As

opposed to cats, in humans, potentials generated by current in the auditory cortices summate at the vertex (Mäkelä et al., 1990).

The MLRs in humans and various mammals have been shown to change with respect to alertness and sleep. In humans, although phases remain stable in different stages of vigilance, the amplitude of the 40 Hz response decreases in sleep (Linden, et al., 1985; Jerger et al., 1986). In addition, in guinea pigs, MLRs have shown marked amplitude fluctuations, being affected by click rate and state of alertness (Kraus et al., 1988). According to the superposition theory, this is significant since changes in MLRs result in changes in the superposition of its waves during ASSR generation. Finally, in cats (Mäkelä, 1990), the optimal stimulation frequencies in obtaining the maximal ASSR were found to be different in changing stages of vigilance.

The 40 Hz ASSR response in humans has been proposed as a result of the coalescence of the MLRs (Galambos et al., 1981; Stapells et al., 1984), where the P_b resonance component in the MLRs is the main contributor to the ASSR resonance. In rabbits (Ottovani, et al., 1990), the superimposing of average 10-Hz potentials were used to synthetize 30Hz ASSRs to be compared with acquired 30Hz ASSRs. The most profound difference found consisted of a phase lead of 45° in the first harmonic with respect to the predicted one. The authors concluded that the aquired ASSRs are likely due to a superposition of ABR and P_b waves, as opposed to a resonance phenomenom. The second study presented in this thesis will test the superposition theory at various rates in guinea pigs.

In a similar study conducted in rats (Conti et al., 1999), synthetic (MLR superposition) and acquired ASSRs were obtained at 30, 40, 50, and 60 Hz. Mean

amplitude calculated on the synthetic ASSRs decreased linearly with increasing stimulation rate and appeared higher in comparison to the acquired ASSRs. Synthetic phases showed a linear increase with increasing stimulation rate and were leading with respect to the corresponding phase values calculated for acquired ASSRs. Thus, the authors concluded that rat MLRs failed to reproduce the amplitude and phase of temporal ASSRs at all repetition rates.

2.3 Generation Mechanisms

There are two underlying theories explaining the generation of the ASSRs, including the linear superposition theory and intrinsic phase synchronization. The first theory**,** which has recently gained more recognition, states that the 40 Hz ASSR response represents the superposition of the MLRs, primarily the P_b component (Bohórquez & Özdamar, 2008).

As discussed earlier, this theory was developed by Galambos, et al. (1981) in order to explain the 40 Hz-ASSRs. The authors concluded that the resulting ASSRs are simply the linear summation of the MLRs evoked by the individual stimuli. This theory gained support from experiments that recorded both MLRs and ASSRs, where the MLRs were shifted and superimposed to closely predict the acquired ASSRs. Furthermore, these results have also been supported in other human (Stapells, et al., 1984; Azzena et al., 1995; Santarelli et al., 1995) and animal (Ottovani et al., 1990) studies.

Most recently, Özdamar and Bohórquez, studied the generation of the 40 Hz ASSR using convolution. With the onset of the recently developed Continuous Loop Averaging Deconvolution (CLAD) method, which allows the acquisition of transient responses at high stimulation rates, the researchers were able to record 40 Hz transient responses (Bohórquez & Özdamar, 2008; Özdamar & Bohórquez, 2006). The researchers demonstrated that the generation of the 40 Hz ASSRs can be reproduced by the superposition of the MLRs at that stimulation rate. It was also reported that the dramatic amplitude increases of the ASSRs at 40 Hz is due to the amplitude increase of the P_b component in the transient response and the corresponding peak alignment (Bohórquez & Özdamar, 2008). My current research encompasses a similar study

performed on guinea pigs to determine if such a phenomenon can be reproduced in mammals.

The second theory proposes that the 40 Hz ASSR is generated intrinsically through the auditory neural network's rhythm, which is believed to be driven by resonators tuned to a frequency of 40 Hz (Basar et al., 1987; Galambos et al., 1982). Thus, it is believed that the resonance is produced when the 40 Hz stimuli activates these resonators. In this theory, the ASSRs are believed to be induced rather than evoked, which is analogous to the phase resetting generation theory of auditory event related responses (Basar,1980; Sayers et al., 1974; Jansen et al., 2003). This theory has more followers from research working on event related potentials and cognitive neurophysiologists.

Other supporting studies have demonstrated the induction of spontaneous and event-related activities in 40-70 Hz range in auditory and other sensory systems (Galambos & Makeig, 1988; Bressler, 1990). Finally, a study by Azzena et al. (1995) found that the linear superposition theory worked only for the 40 Hz ASSRs, but not for other repetition rates (7, 9, 20, 50, 60 Hz). They concluded that the ASSR generation depended on the recovery cycle related mechanisms and the resonant frequency property of the sytem. It is important to note that since there is no concrete physical model to test the intrinsic phase synchronization theory, quantitative studies have yet to be conducted at this time.

In addition to allowing for us to gain further understanding over the distinctions of the human and mammal auditory response, this research could allow for the potential use of animals in place of human studies. For instance, if it is found that the guinea pig

and human response share very similar characteristics, anesthesia studies could then be conducted on animals and not humans. These would allow for studies to be more cost-effective, versatile, and easier to conduct. Similarly, neurocognitive studies involving evoked and induced potentials and brain oscillations could be conducted on awake, trained animals revealing more details about the generation mechanisms.

CHAPTER 3: METHODS

3.1 Surgical Procedure and Recordings

The surgical procedure and recordings of the guinea pigs were performed in the summer of 2007 in Ankara, Turkey. Prior to surgery, the guinea pigs were given vitamin C and fresh green vegetables as a means of reducing stress. In addition, proper antiseptic measures were taken to prevent infections. The surgery time was between 1.5-2 hours and was performed on animals weighting 550-1050 g. At least one week prior to physiological recordings, chronic electrodes were implanted as follows.

Ketamine (100 mg/kg) and Xylazine (4 mg/kg) were administered intramuscularly to induce anesthesia. In addition, a local anesthetic was utilized at times if the animal displayed any discomfort. After sedation, the animal's head was shaven with a disposable razor in order to expose the head region. Next, the animal was placed on the stereotaxic operating equipment, ensuring the body was elevated and the mouth restrained to minimize neck discomfort. In order to create a more stable operating environment, ear bars were adjusted until the head was held firmly in place. Special care was taken to ensure that the steel bars were not pressed deep into the ear channel to avoid damaging the animal's hearing.

After the animal was stabilized, an incision was made through the scalp from the occipital to the frontal region of the head. Next, using a fine tip permanent marker, specific points were labeled and drilled (0.85 mm diameter) as shown in **Figure 3.1**. Stainless steel screw electrodes (1mm diameter) were then screwed into each of the marked holes.

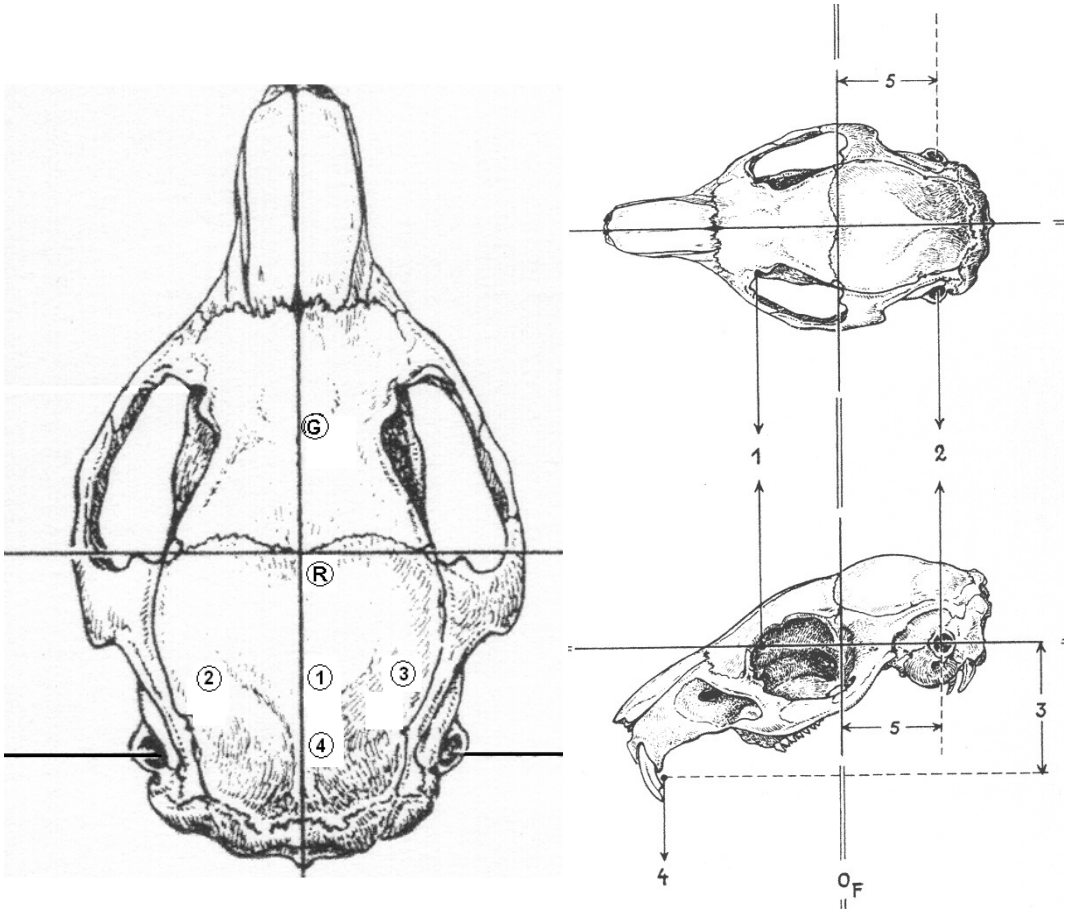

Figure 3.1. Guinea pig skull (Rossner, 1965) with labeled drilling points. R: reference; G: ground; 1 and 4: central positions; 2 and 3: temporal positions.

The next step was to prepare the dental acrylic mixture by mixing two reacting compounds. An initial conservative amount of dental cement was applied to cover the incision and screws, while ensuring that that the end of the wires extended above the cement for soldering to a 9-pin socket. Using a wire stripper, the insulation from each of the cables was stripped to expose the bare wire tip. Each wire was then soldered to its respective pin of a 9-pin, gold coated socket. In order to ensure the connections were made correctly, a multimeter was used to check for short circuits. Special care was taken to apply antibiotic ointment on the wound to avoid infections.

The final step in the surgery was to apply the final layers of dental cement in order to affix the electrodes, cables, and connection socket to the skull. Before the cement dried, the animal number was marked on the cement base and a small steel cylinder was placed across the front of the cement base.

3.2 Data Acquisition

The still and calm nature of the guinea pigs generally allows for artifact-free recordings in an awake state. However, the guinea pigs were retrained in order to minimize any major movements. The animal was not anesthetized during recordings due to its affect on the MLRs of a transient response.

Table 3.1 lists the guinea pig (GP) # and session # for all the animals. Since the amount and type of data for each animal is different, not all of the animals were included in this research. Overall, the data from 6 animals are reported, with 3 of the animals tested in two sessions as shown in the table.

Table 3.1. Guinea pigs (GP) and sessions recorded data.

GP #	SESSION #
57	12
60	10, 26
61	7

GP #	SESSION #
62	8
63	20, 25
68	1, 13

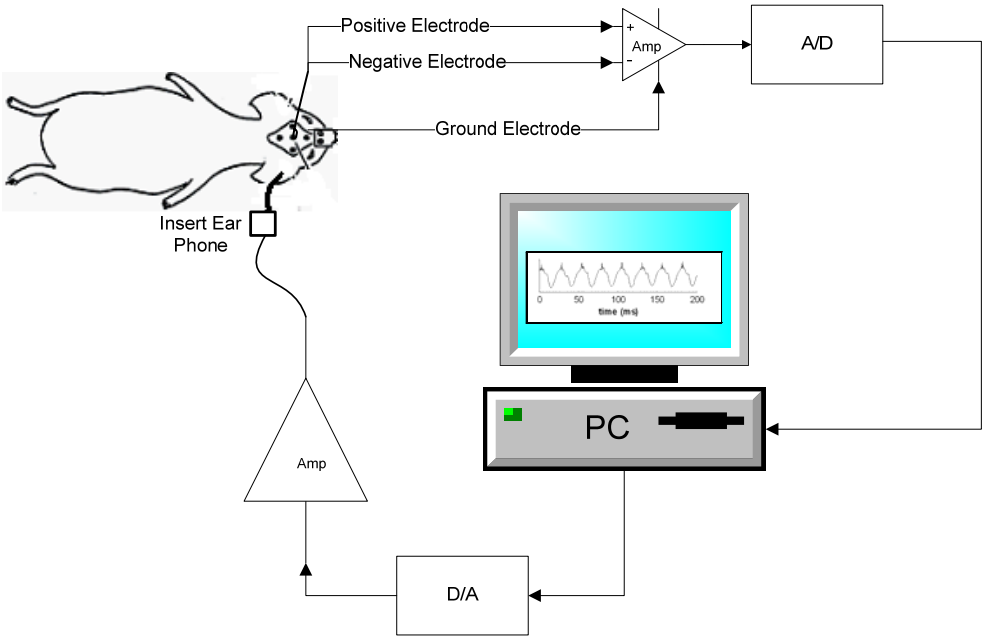

Figure 3.2. Schematic showing a typical guinea pig auditory recording system.

Figure 3.2 shows a schematic of the set-up used for obtaining AERs in guinea pigs. The results in this study were carried out in an anechoic, sound-attenuated, dim, electrically shielded electrophysiological recording booth. Insert type earphones (Biologic 21110) were used to apply 100 ms, 70 dB clicks. The recordings were obtained using the SmartEP system (Intelligent Hearing Systems, Miami, FL) amplified (gain: 100,000), band pass filtered (10-1500 Hz, 6 dB/oct) and digitized at 100xN µs (multiples of 100µs) sampling time. Data was collected using three conventional (2.5, 5, 10) and six CLAD sequences (14.7, 19.5, 26.9, 39.1, 61.0, and 78.1 Hz). As shown in **Table 3.2**, each sweep consisted of 1024 data points with duration of 204.8-819.2 ms. Artifact refection was set to 20 microsec and 256 sweeps were averaged for each recording. In order to unwrap these overlapping data, it was deconvolved offline using the frequency domain CLAD method (Özdamar and Bohórquez, 2006) implemented in a Delphi program. For this study, the results centered on four stimulus sequences at 20, 40, and 80

Hz, including: low jitter (40Narrow), low-medium jitter (80OPtim), and medium jitter (Bi08). **Figure 3.3** displays the time and frequency transfer characteristics of the sequences used in this study. As seen from the frequency characteristics, all three sequences are specially designed to minimize any noise amplification (>1 horizontal line) as specified for the CLAD deconvolution algorithm (Özdamar & Bohórquez, 2006).

Table 3.2. Recording Parameters of guinea pig recorded data.

STUDY	Ear	Int (dB)	Rate (Hz)	sweeps	Sampling (ms)	Sweep Length (ms)
TRANSIENT	Right	70	**2.44-156.25**	256	100-800	102.4-819.2
STEADY	Right	70	**2.44-156.25**	256	100-800	102.4-819.2

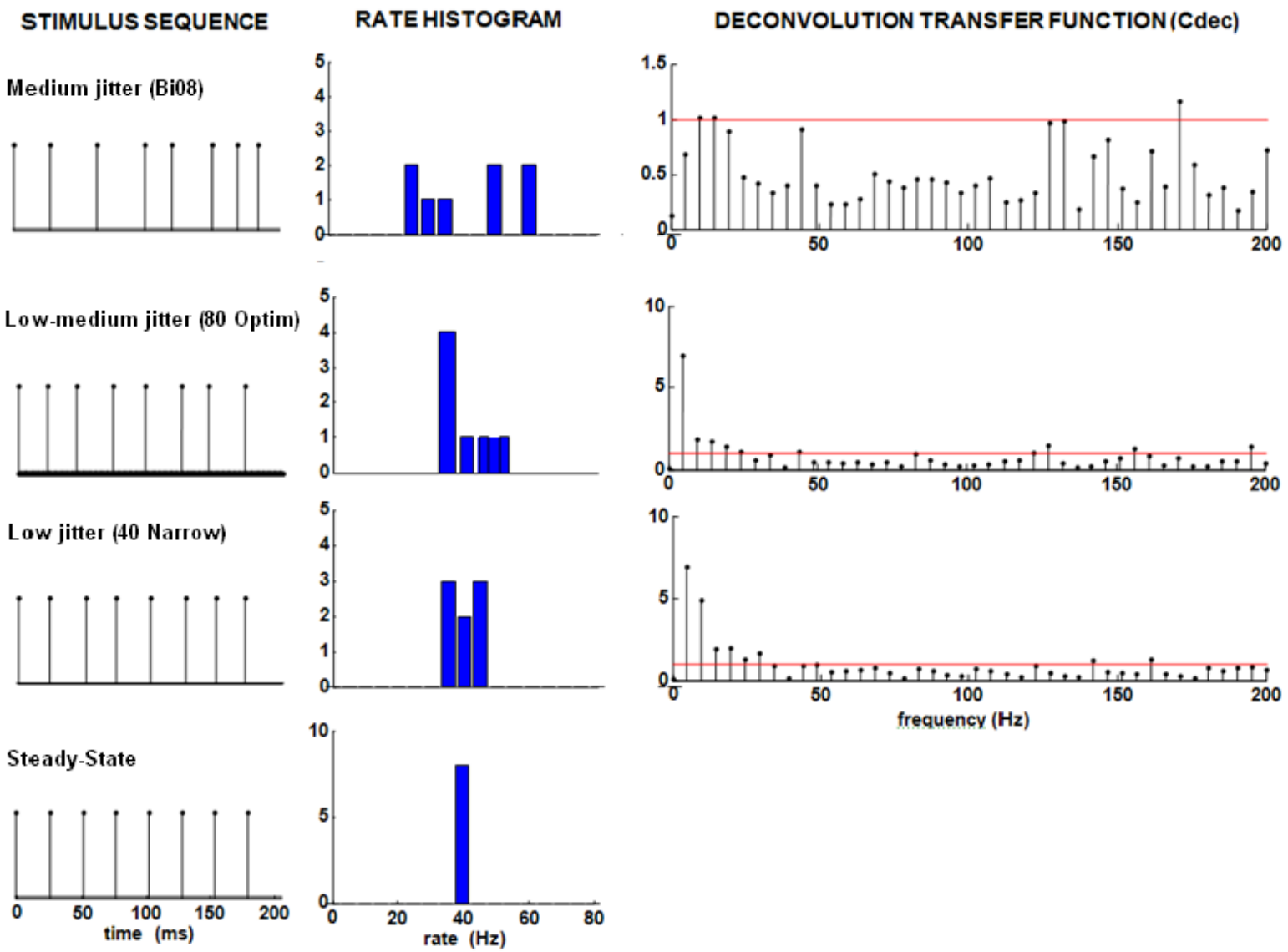

Figure 3.3. Stimulus sequences with rate histogram and deconvolution transfer function (modified from Bohórquez, personal communication)

After providing the stimuli sequences to the animal, the brain generates an evoked response, which is embedded in the collected EEG data. As shown in **Figure 3.4**, sweep averaging is used to reduce the EEG portion, leaving the convolved AER with residual noise. This averaging method was used to obtain both the ASSRs and transient responses.

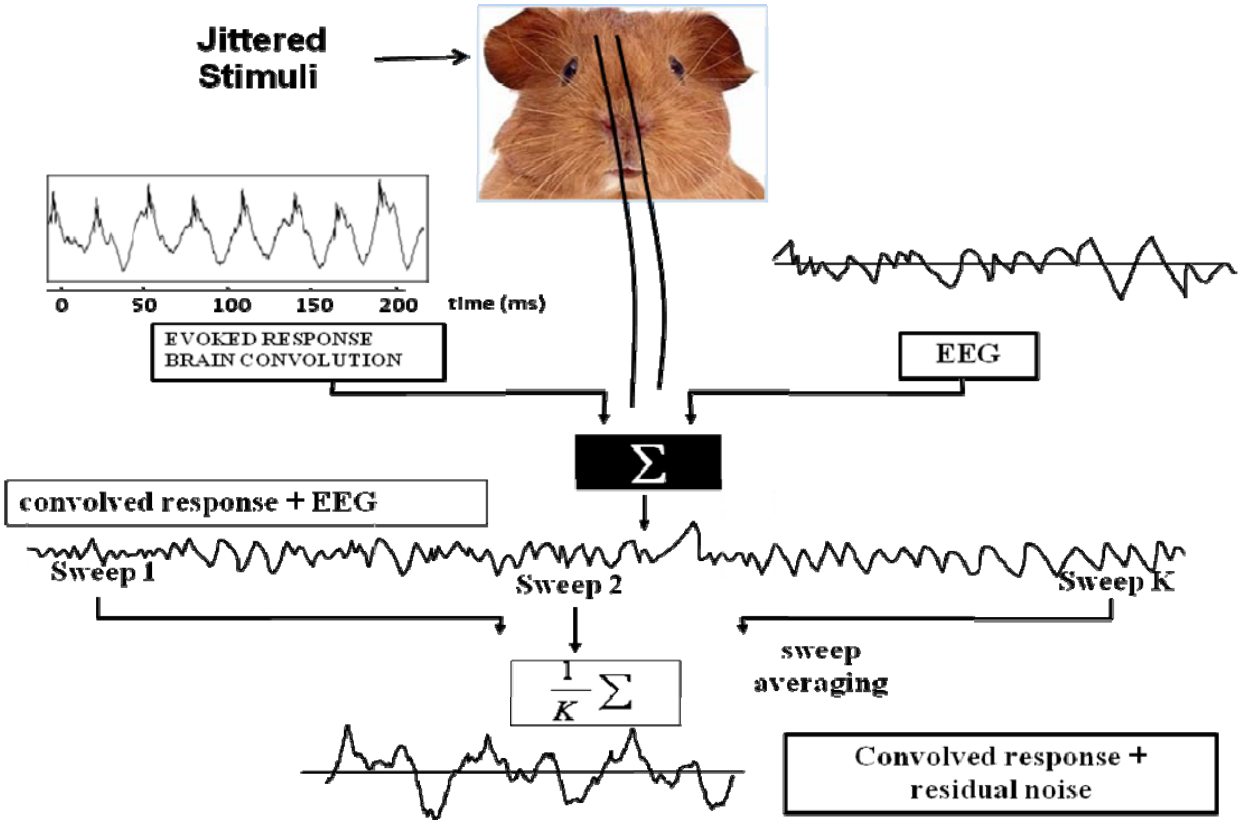

Figure 3.4. AER recording procedure used in guinea pigs.

3.3 40Hz ASSR Resonance Study

The first part of this research involved studying the presence of an ASSR resonance at different rates. After plotting the ASSRs at increasing rates, ASSRs peak-to-peak amplitudes and ASSRs peak-to-peak fundamental frequency amplitudes as a function of rate were analyzed. In addition, the grand average (population average) and normalized grand average of the ASSRs peak-to-peak and peak-to-peak fundamental frequency amplitudes were used to further investigate the presence of a resonance. The entire process is summarized in the figure below (**Figure 3.5**).

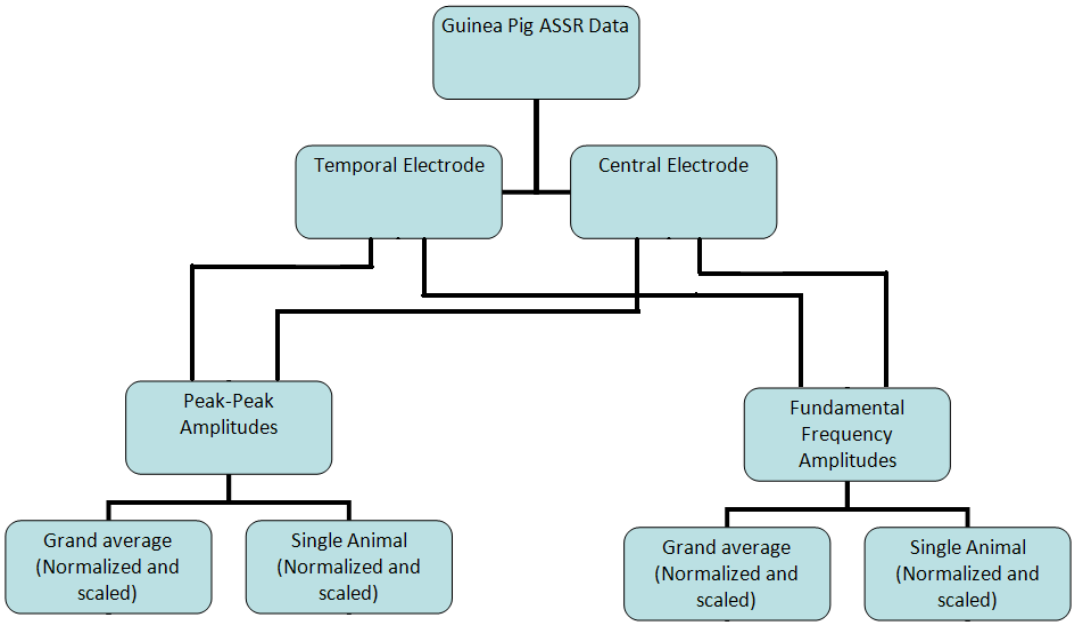

Figure 3.5. Flowchart showing the procedure used in analyzing the resonance characteristics of the ASSRs.

Three Matlab programs were written to determine quantitatively the possible resonance effects. The first program (plot_ASSRs.m) was designed to plot all the ASSRs for any of the animal sessions. The program simply required the user to input the animal

session and it then automatically plotted the ASSRs by ascending stimulus rate. This allowed for the initial visual inspection to observe any increases in amplitudes.

The second program (Amplitude_study.m) was designed to plot the peak to peak amplitude of the ASSRs at various rates for each animal session. This plot provided a valuable visualization tool to more objectively determine any possible resonance in the results. It is important to note that the peak to peak amplitudes were calculated for the denoised ASSR, which contained only the three main harmonics. This procedure did not compromise the data since the signal energy is confined to the main frequency and its harmonics. The program also had the option of studying the data using only the fundamental frequency amplitudes. Since the original data can sometimes be distorted, studying the fundamental frequency of the ASSRs eliminated this problem. Thus, the fundamental frequency amplitude plots provided another tool to verify the presence of a resonance.

One of the most critical aspects in this study was the conglomerate effects of all the animal recordings. The task proved to be quite lengthy since it involved analyzing all of the animals' data and determining all the matching parameters to properly average the data. After finding the matching rates for all the animals, a third program (Superaverage_amplitude.m) was written to perform the grand average of both peak to peak amplitudes and fundamental frequency peak to peak amplitudes. Finally, the user is given the option of viewing the results in logarithmic scale, which allows the user to view possible significant changes in amplitude otherwise dismissed in regular plots.

3.4 Simulation of ASSRs

The second part of this study involved comparing the acquired ASSRs with synthetic ASSRs generated from transient responses. This step is crucial since it was recently discovered in humans that the 40 Hz ASSR could be synthetically generated by the superposition of the major waves of the ABR and MLR (Bohórquez & Özdamar, 2008). Thus, this part of the study will determine if this phenomenom is shared in other mammals. The comparison will be measured using various methods, including: correlation coefficient and phasor analysis.

In order to generate the synthetic ASSR, jittered stimuli were used to obtain quasi ASSRs. Quasi ASSRs are simply the result of the overlapping of MLRs, which gives the visual appearance of regular acquired ASSRs. In order to test the superposition theory, the quasi ASSRs were first separated into its individual transient responses by applying CLAD (**Figure 3.6**).

Once the transient responses were attained, proper convolution was performed in order to simulate the synthetic ASSRs. **Figure 3.7** shows the convolution process, which involves using cyclical time shifted MLR waveforms. In this step, the MLR waveforms were divided into 8 segments and time shifted 25.6 ms to generate 8 consecutive recordings, which were wrapped around to form a continuous loop. These newly created recordings were then added to generate the synthetic ASSR.

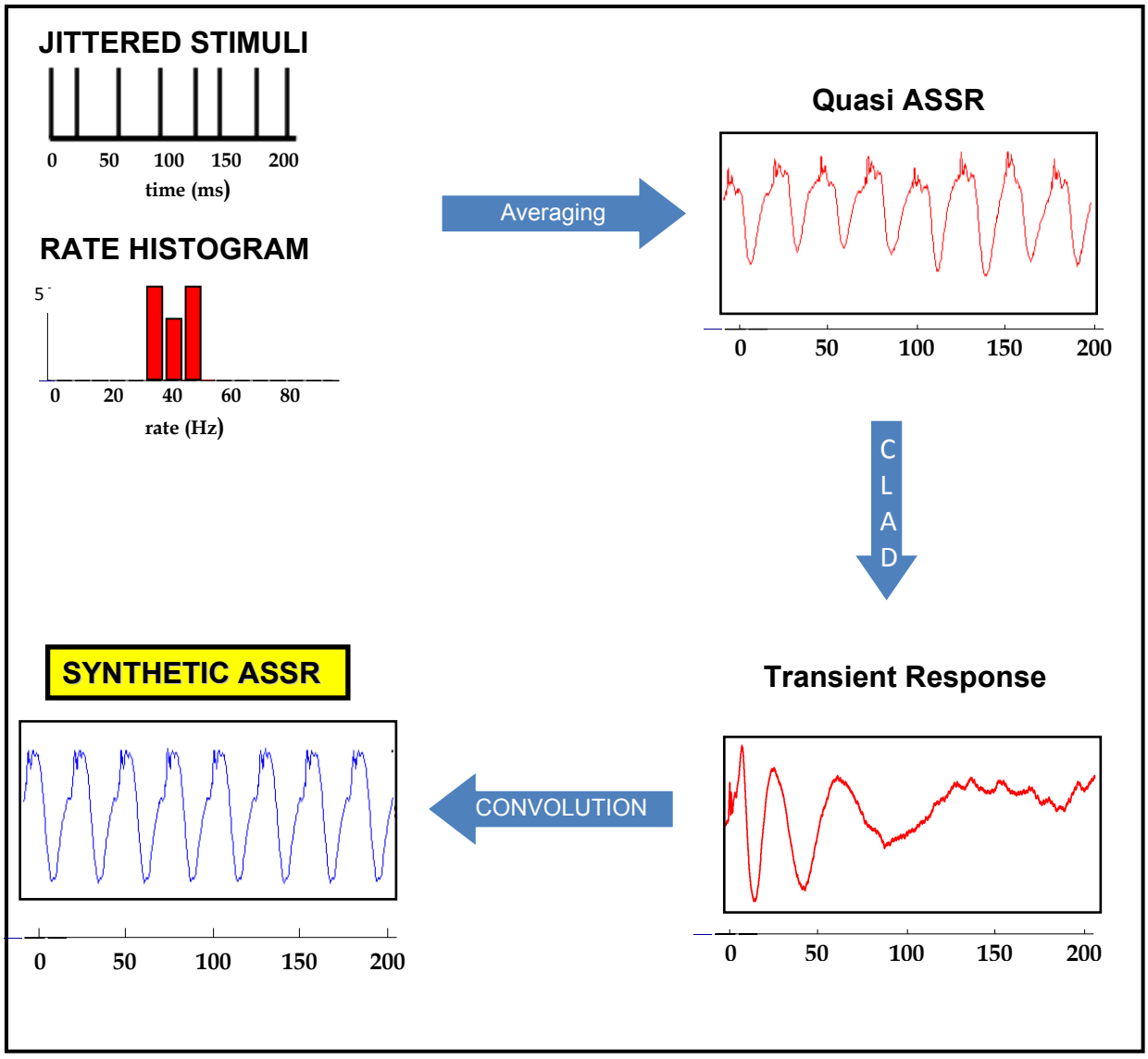

Figure 3.6. Schematic flowchart of the procedure for obtaining quasi ASSR and synthetic ASSR.

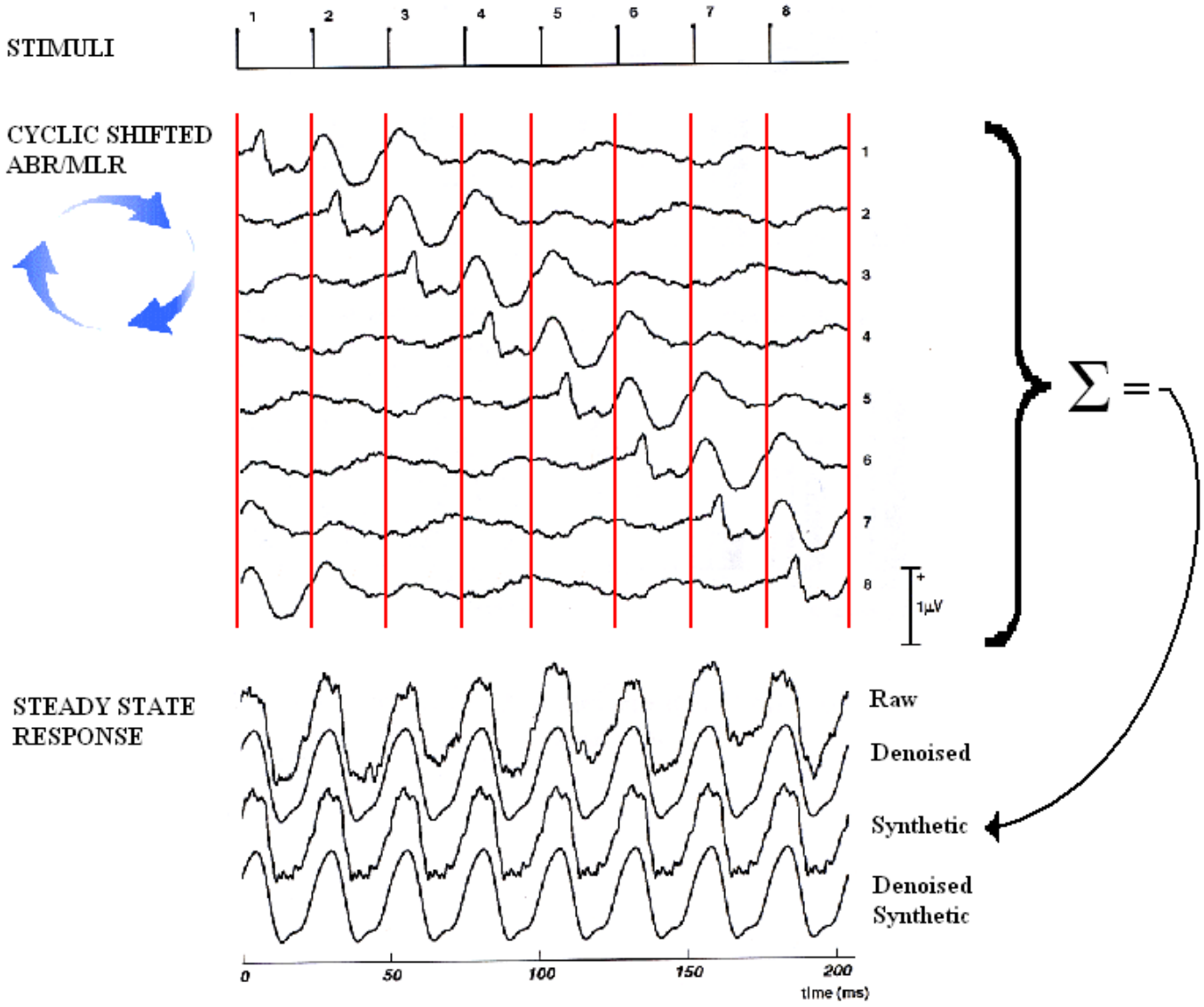

Figure 3.7. Synthetic ASSR generated by convolution and compared to the acquired in both raw and denoised forms (modified from Bohórquez & Özdamar, 2008).

3.5 Acquired vs. Synthetic ASSR Study

This part of the project involved the comparison of the synthetic and real ASSRs through correlation coefficient and phasor analysis (**Figure 3.8**). The resulting data was then categorized based on the sequence used to generate the responses. Two programs were written for the comparison of the responses, with one focusing on the correlation coefficient (Correlations.m) and the other on the phasor analysis (Phasor_Final.m).

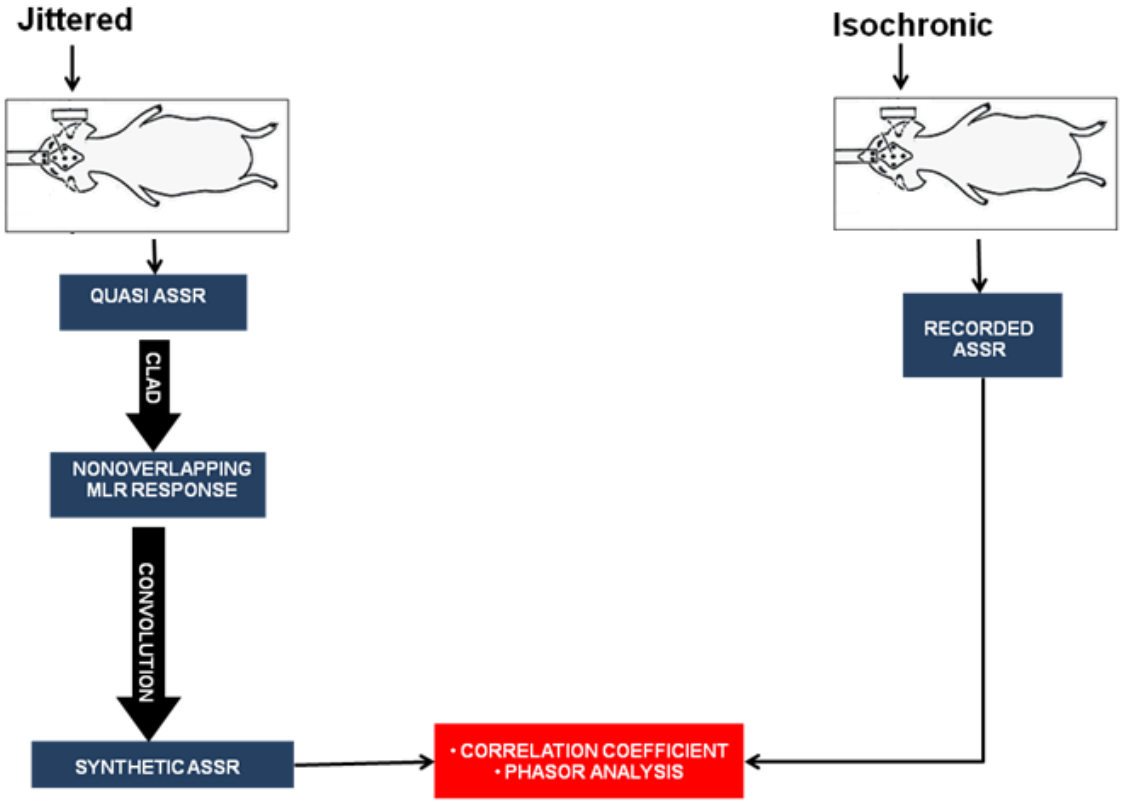

Figure 3.8. Correlation coefficient and phasor analysis comparison analysis.

The first program (Correlations.m), which plots the subtraction of the signals and computes the correlation coefficient, uses interpolation prior to the comparison of the data due to differences in sampling time. This matching in sampling time is required

prior to subtracting the responses and calculating the correlation since it requires point by point computations. For example, an acquired ASSR is recorded at a sampling rate of 5000 Hz for a total of 1024 points, yielding a sweep time of 200 ms and a sampling time of 200 μs. On the other hand, a transient ASSR, yielding the synthetic ASSR, is recorded at a sampling rate of 1250 Hz for a total of 1024 points, yielding a sweep time of 800 ms and a sampling time of 800 μs. The Matlab program utilized in this study uses interpolation to automatically adjust the synthetic ASSR sweep time to 200 ms and sampling time to 200 μs to match the acquired ASSR parameters, while maintaining the 1024 points. This program then plots the difference of the two responses and computes the correlation coefficient.

One of the disadvantages with utilizing the correlation coefficient is that it disregards amplitude differences in the signals. It simply compares the normalized versions of the responses, which results in the lost of the magnitude portions of the responses. Plotting the difference between the responses helped to visually observe any changes in amplitude, but it still failed to provide a quantitative factor needed in comparing large amounts of data.

Thus, in order to circumvent these problems, a phasor analysis was implemented to more closely study the differences in the signals. Phasors interpret a signal in phase and magnitude, allowing for an analytical comparison of both shape and amplitude between the two signals. This method is ideal since a steady-state response, which is periodic, can be fully described in phasor plots.

The second program (Phasor_Final.m) used phasor analysis in the comparison to the two signals. In order to prevent the development of small spurious peaks through the

superposition of the MLR responses, the synthetic ASSR was comb filtered to keep only the three main harmonics. Thus, for the 40 Hz response, the main harmonics were f_0=39.60 Hz, f_1=78.12 Hz, and f_2=117.18 Hz. The same filter was applied to the acquired ASSRs so that the signals could be compared at each of the three main harmonics.

In order to apply the comb filter discussed above, it is important to understand that a signal can be viewed in both time and frequency domain. Although both versions are useful, one can be more beneficial depending on what we want to do with the signal. In this case, since the analysis revolved around ASSRs, the frequency domain is the best option, since it allows the signal to be viewed in terms of magnitude and phase. The Discrete Fourier Transform (DFT) is a form of Fourier analysis that converts a time-domain signal into frequency domain. It is widely used in signal processing to analyze frequencies in a signal and perform convolutions. However, as samples reach realistic numbers, the number of calculations involved are enormous, which is unappealing to most. Fortunately, Fast Fourier Transform (FFT) offers a simple and efficient method of computing the DFT. The Inverse Fast Fourier Transform (IFFT) is simply a method of converting a signal back from its frequency domain into its time domain. The acquired and synthetic ASSR data generated were filtered using FFT and IFFT. After performing the FFT of the signal, the trivial frequencies were eliminated, leaving only the first three harmonics, followed by the IFFT of the signal for conversion back to time domain. Thus, in the case of the 40 Hz response, the harmonics were f_0=39.60 Hz, f_1=78.12 Hz, and f_2=117.18 Hz. This method does not compromise the data since the signal energy is confined to the main frequency and its harmonics. This program computes both the magnitude and phase of the signals for the three main harmonics and plots it as phasors.

The program also outputs for each signal the SSR harmonic magnitudes, phase, and RMS error at each harmonic, which can then be easily imported into excel for analysis.

Figure 3.9 shows an example of the acquired (blue) and synthetic (red) response in both time domain (left) and first harmonic phasor representation (right). A quick observation shows that the phases have only a small margin of error and the magnitudes differ by about 0.15 μV.

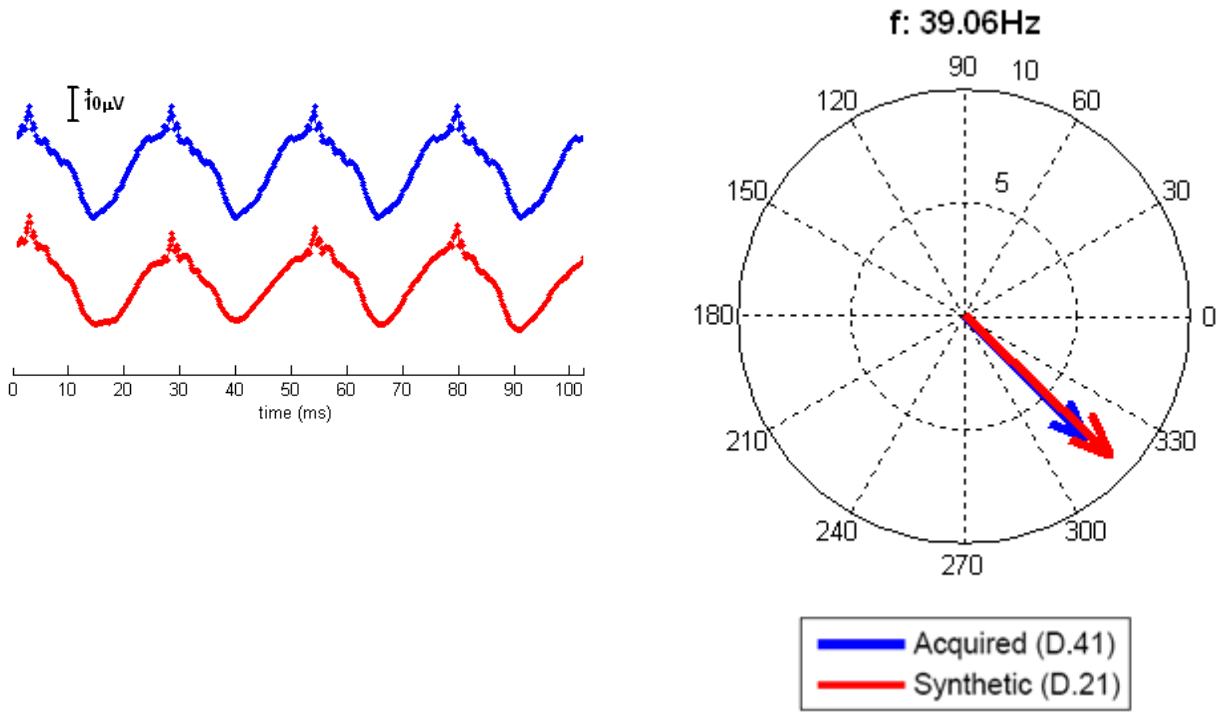

Figure 3.9. Left plot shows the acquired (blue) and synthetic (red) 40Hz ASSR signals in time domain representation. Right plot is the first harmonic phasor representation of the same responses.

In order to analyze the information of all the animals, the grand average (population average), of both amplitude and phase were computed and compared for each of the three sequences at 20, 40, and 80 Hz. Finally, the mean prediction error for each

sequence was plotted to further study the effects of stimulation sequence on ASSR prediction.

CHAPTER 4: RESULTS AND DISCUSSIONS

4.1 ASSR Characteristics as a Function of Rate

The first part of this research investigated the presence of an ASSR resonance by studying the effects of rate on the response. First, ASSRs peak-to-peak amplitudes and ASSRs peak-to-peak fundamental frequency amplitudes at the various rates were plotted for both temporal and central electrodes. In addition, the grand average and normalized grand average of the ASSRs peak-to-peak and peak-to-peak fundamental frequency amplitudes were plotted to examine the conglomerate effects of all the animal recordings.

Figure 4.1 shows the grand average plot of the guinea pigs' ASSRs at the specified rates for six guinea pigs. **Figure 4.1A** displays the peak to peak amplitude of the denoised response and represents the most direct way of determining any resonance. Since ASSRs tend to contain noise, plotting the fundamental frequency amplitudes (**4.1B**) allows us to study the general trends present in waves, while minimizing the noise that often accompanies them. In the temporal electrode, both plots clearly demonstrate a normal distribution shape with a resonance near the 40 Hz region. Five of the six guinea pigs were tested at other rates as well. **Figure 4.2** demonstrates the results at many more rates, albeit with one less guinea pig included. This guinea pig (Session # 01) was excluded because the tests conducted on the animal contained only the basic stimulation rates shown in **Figure 4.1**. **Figure 4.2** again clearly confirms the results, showing a resonance near the 26-52 Hz region for both ASSR peak to peak and fundamental frequency amplitudes in the temporal electrode. Overall, the temporal electrode 40 Hz resonance can be observed in guinea pigs, but it appears somewhat broad and flat.

As shown in both figures, the centrally recorded ASSRs are smaller and tend to have resonances at higher rates when compared to temporal signals. This observation can be seen in both peak to peak and fundamental frequency amplitudes.

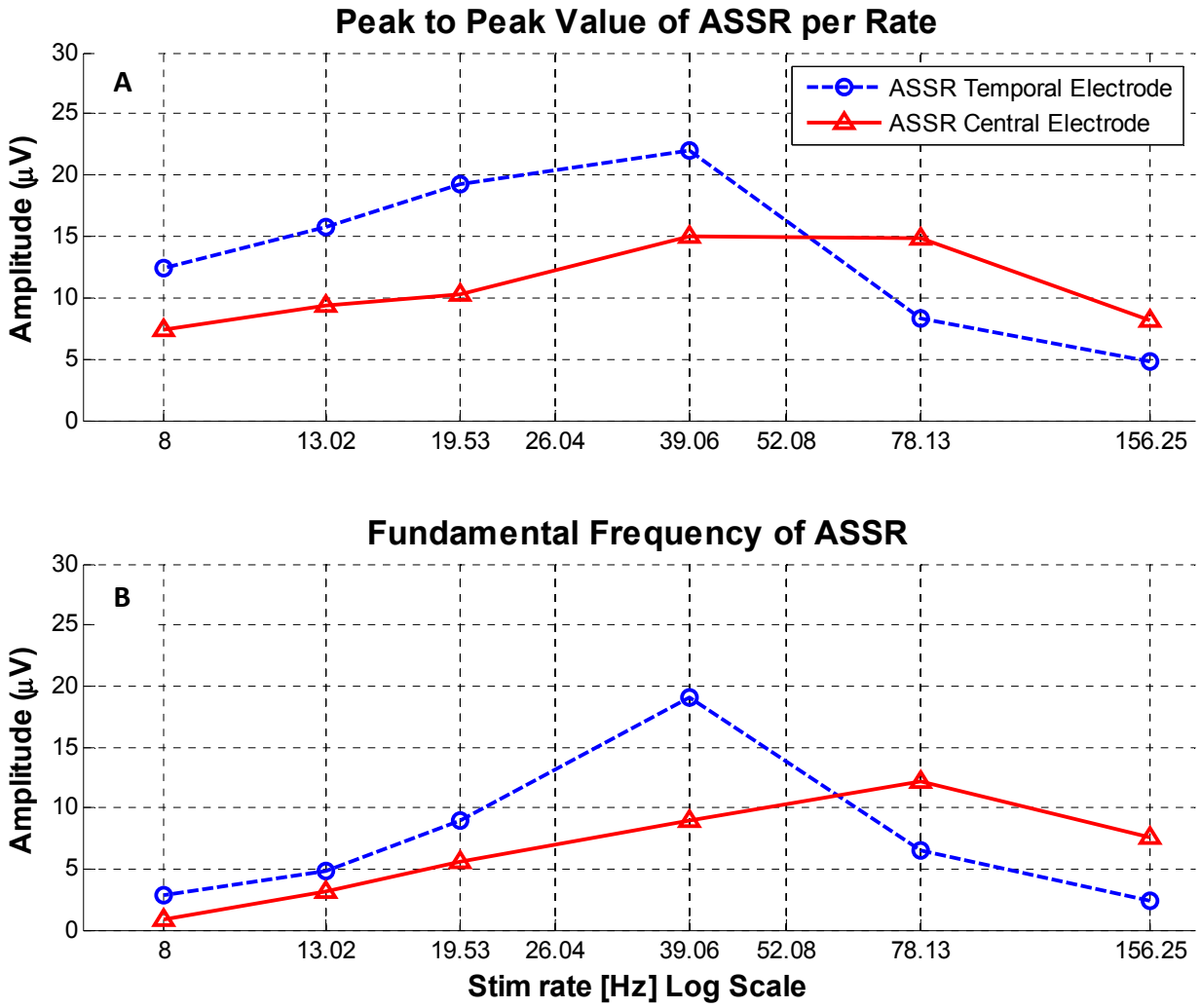

Figure 4.1. Grand average of the averages of measured amplitudes of six guinea pigs (Session # 01,07,8,10,12,13) ASSRs with respect to rate. Top (A) shows peak to peak amplitude of the denoised response, containing the three main harmonics. Bottom (B) shows the fundamental frequency amplitude. Temporal and central electrodes are shown independently.

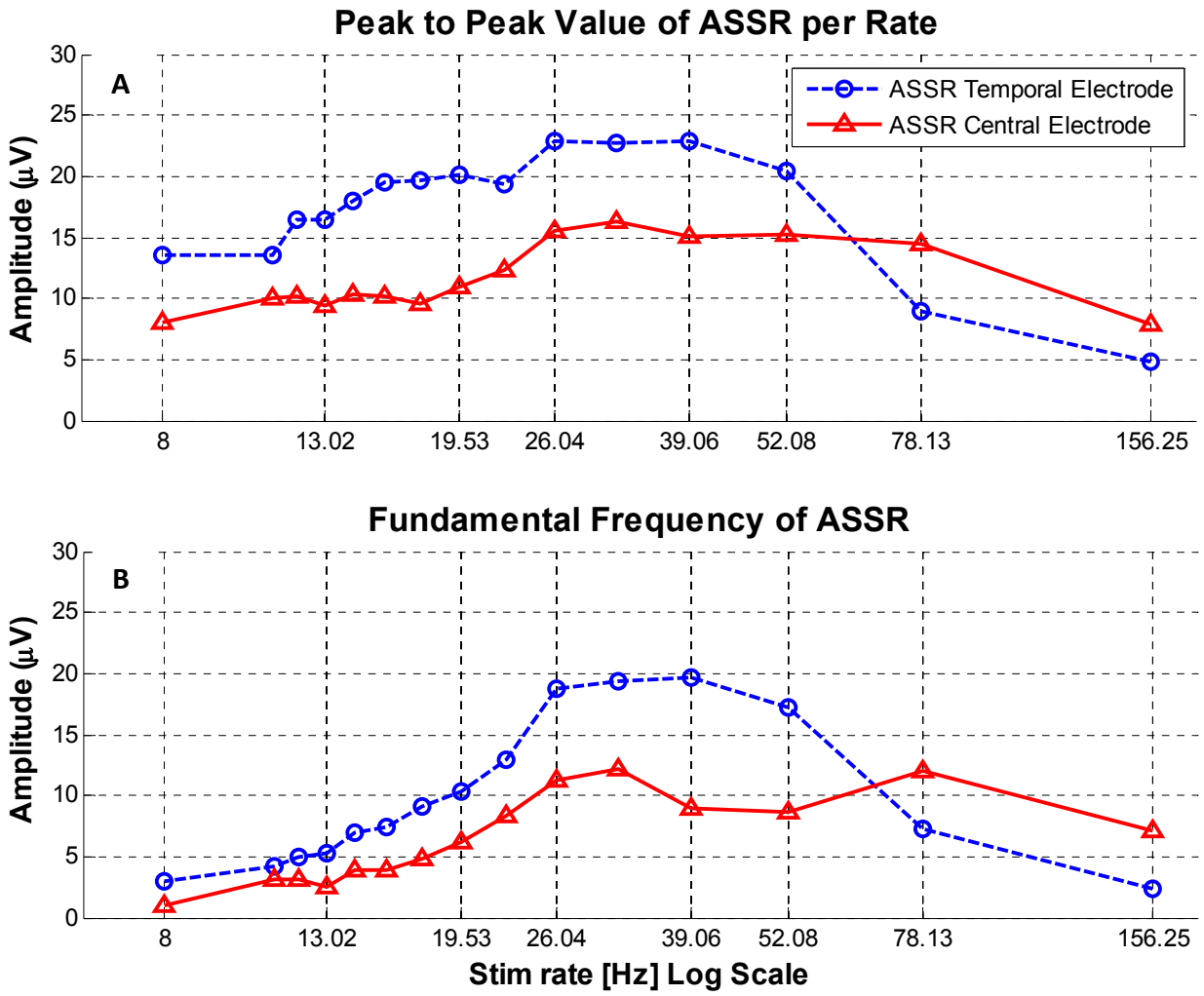

Figure 4.2. Grand average of the averages of measured amplitudes of five guinea pigs (Session # 7,8,10,12,13) ASSRs with respect to rate. Top (A) shows peak to peak amplitude of the denoised response, containing the three main harmonics. Bottom (B) shows the fundamental frequency amplitude. Temporal and central electrodes are shown independently.

It was observed that the amplitudes of the individual animals' ASSRs differed greatly, sometimes by a factor of four. Such high variability among animals could potentially obscure the grand average results, since the process involves the average of the amplitudes of all animals at each of the rates. Thus, to address this issue, the above data were normalized with respect to each animals' highest amplitude measurement and plotted. **Figure 4.3** shows the results for six animals at six rates, while **Figure 4.4** shows the results with more rates in five guinea pigs. Once again, the plots show a resonance around 40 Hz and a general normal distribution for the temporal electrode. As for the central electrode, the recorded ASSRs show a resonance at higher rates compared to temporal signals.

The results of this research seems to be somewhat in parallel with the human 40 Hz ASSRs resonance studies. Human ASSR resonance, however, is more narrowly tuned around 40 Hz than the guinea pig ASSR, which is very broadly tuned. Also, human ASSRs are highest at central positions, while guinea pig ASSRs are highest in the contralateral temporal position, as confirmed in other guinea pigs (Yoshida et al., 1984), cats (Mäkelä et al., 1990) and rats (Conti et al., 1999).

In a recent study by Demirtas and Özdamar (2008), the effects of high stimulus rate of guinea pig auditory evoked potentials were studied using high rate click in awake animals (2.5-78.1 Hz). The study found that the latencies of the four waves (0, A, B, and C) varied, but had no significant changes. In addition, although the amplitude of wave A, B, and C decreased gradually with increasing rate, the amplitude of Wave C showed a slight but small increase at around 39.1 Hz. These results are somewhat similar to those in the human auditory system, which shows a dramatic increase of the Pb component.

The P_b wave is said to correspond to the Wave C in cats (Buchwald et al., 1981) and possibly . Thus, the small resonance at around 40 Hz in guinea pigs may be accounted by this slight MLR increase as in human ASSRs (Bohórquez & Özdamar, 2008). Thus, it can be argued that the slight resonance in the transient responses (Wave C) is responsible for the 40 Hz ASSRs resonance found in this study.

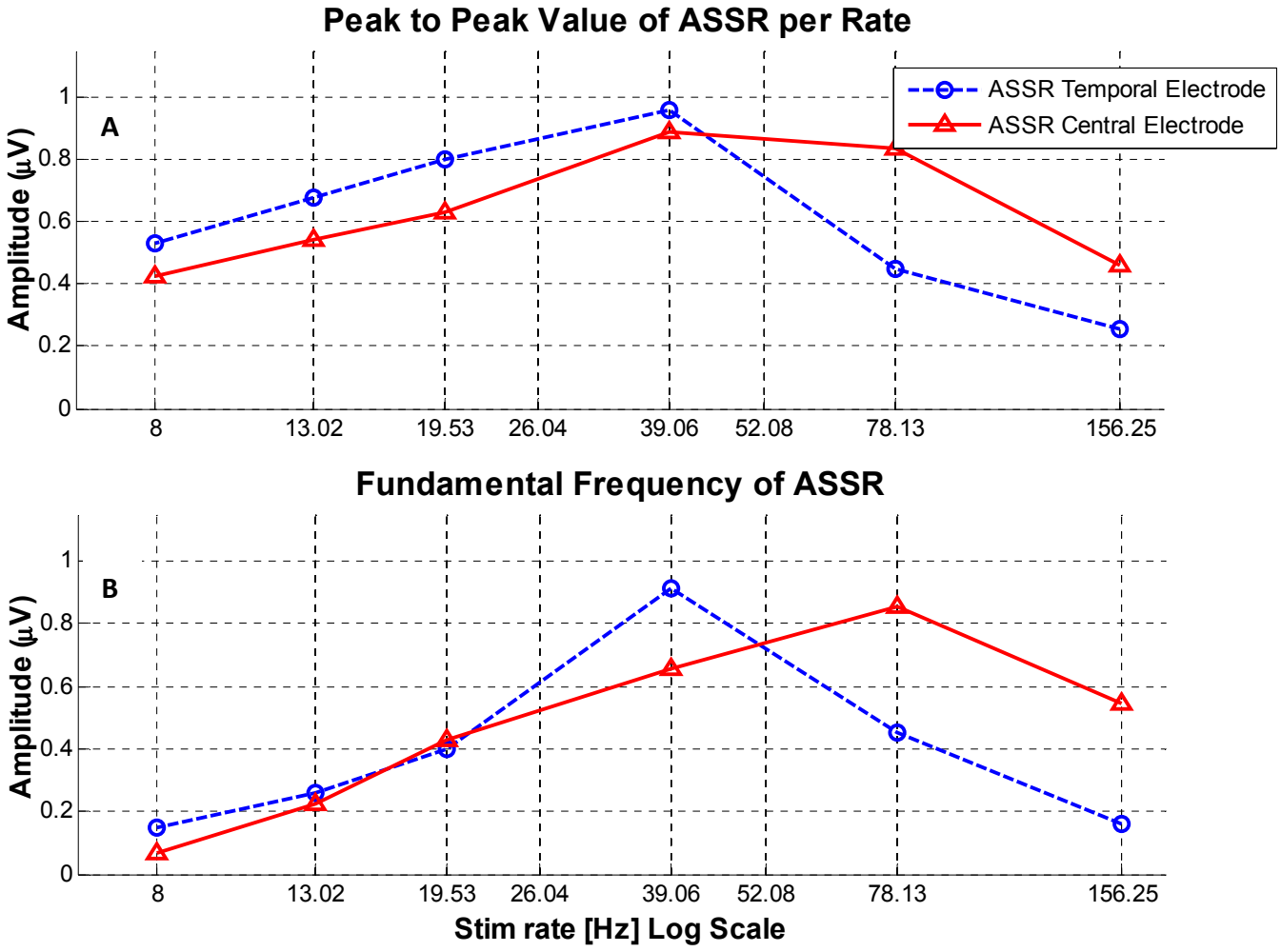

Figure 4.3. Normalized grand average of the averages of measured amplitudes of six guinea pigs (Session # 1,7,8,10,12,13) ASSRs with respect to rate. Top (A) shows peak to peak amplitude of the denoised response, containing the three main harmonics. Bottom (B) shows the fundamental frequency amplitude. Temporal and central electrodes are shown independently.

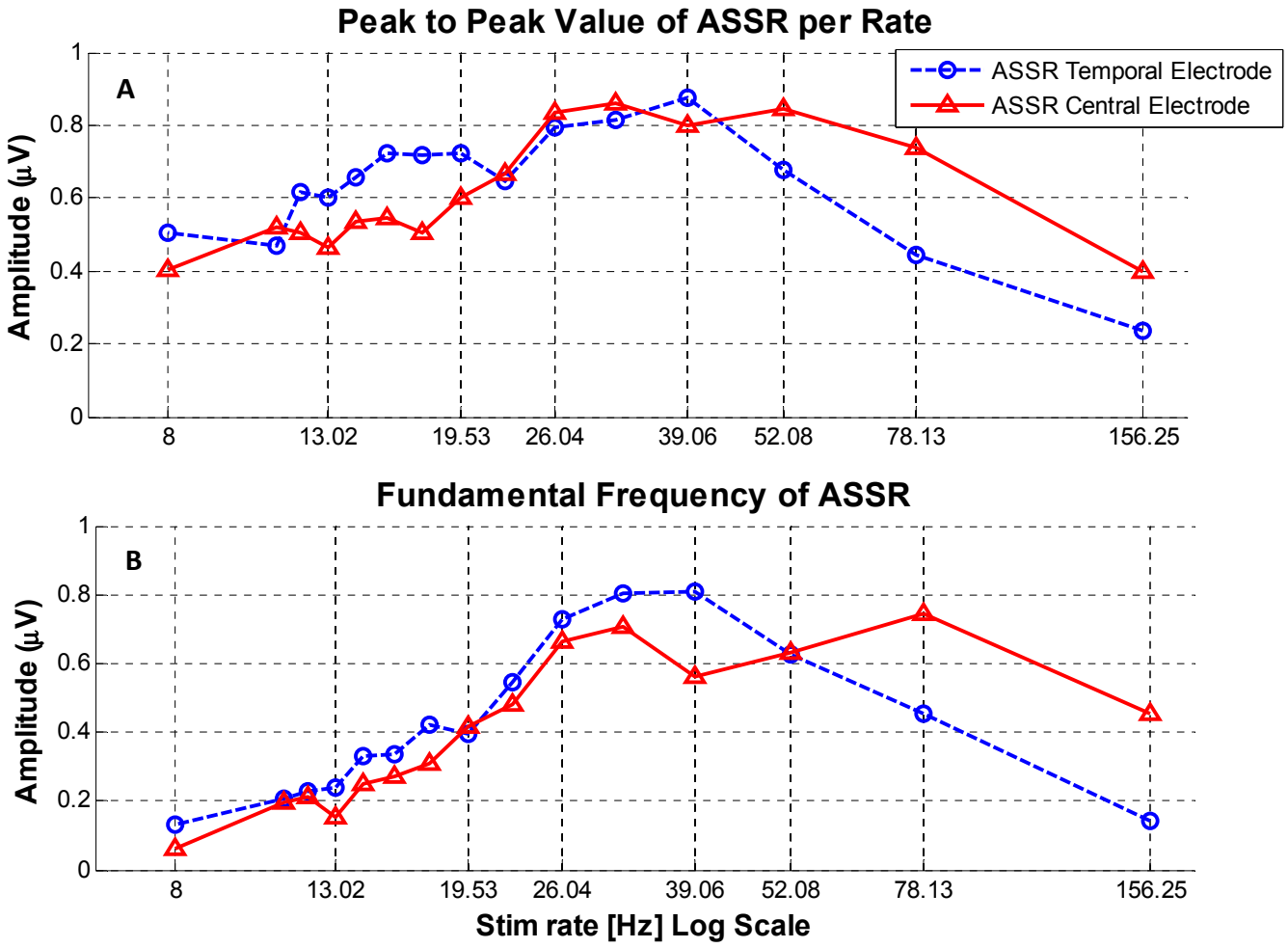

Figure 4.4. Normalized grand average of the averages of measured amplitudes of five guinea pigs (Session # 7,8,10,12,13) ASSRs with respect to rate. Top (A) shows peak to peak amplitude of the denoised response, containing the three main harmonics. Bottom (B) shows the fundamental frequency amplitude. Temporal and central electrodes are shown independently.

4.2 Acquired vs. Synthetic ASSR Results

In the second part of the study, the superposition theory of the 40 Hz ASSR was tested by computing the synthetic ASSR and comparing it to the acquired ASSR through two distinct ways: correlation coefficient and phasor analysis. The resulting data were then categorized and interpreted based on the sequence used to generate the responses. The following sequences were used in this study: low jitter, low-medium jitter, and medium jitter.

4.2.1 Cross Correlation Coefficient

The first method used to compare the acquired and synthetic signals at 20, 40, and 80 Hz was the correlation coefficient. As warned earlier, this method normalizes the signals during comparison, leaving the signal shape as its only comparison factor. Consequently, a visual inspection of the two signals did reveal some minor amplitude differences.

Comparison at 40 Hz rate

The grand average of the cross correlation between the acquired and synthetic ASSR data from five animals are plotted in **Figure 4.5**. In the temporal electrode, all the three sequences generated a correlation coefficient above 0.8. Overall, low jitter is best, followed by low-medium jitter and medium jitter. These results demonstrate that at 40 Hz in the temporal electrode, low and low-medium jitter sequences better predict the acquired ASSRs than medium jitter sequences.

The results for the central electrode at 40 Hz are fairly consistent at all sequences, with values above 0.8. Thus, at 40 Hz, in the central electrode, all sequences appear to predict the acquired ASSR to a similar degree. However, as in the previous cases, the less jittered sequences better predict the acquired response.

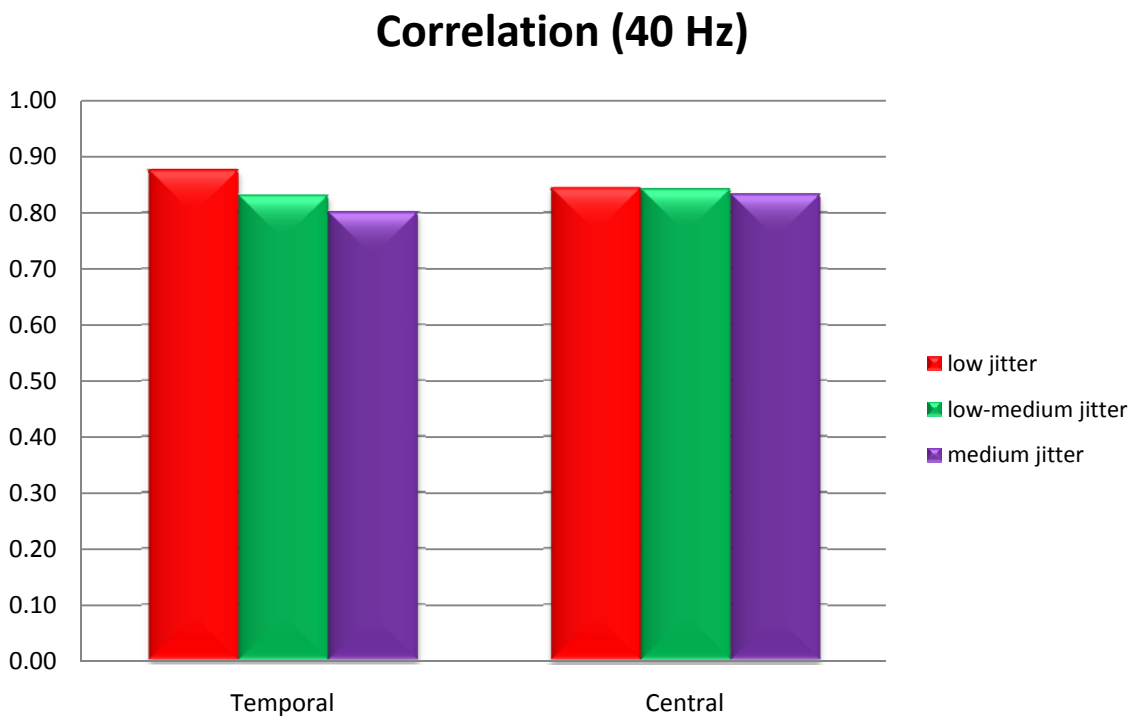

Figure 4.5. Mean correlation coefficient for five guinea pigs (Session # 10, 12, 13, 25, 26) at 40 Hz between the acquired and synthetic ASSRs for three sequences in the temporal and central electrodes.

Comparison at 20 Hz rate

As shown in **Figure 4.6**, in the temporal electrode, all the three sequences show a correlation coefficient above 0.85. The best sequence is low jitter, followed by low-medium jitter and medium jitter. Similar to the 40 Hz temporal electrode, lower jitter sequences at 20 Hz better predict the acquired response than medium jitter.

The results for the central electrode showed a lower correlation coefficient, with values around 0.70. The low jitter sequence best predicts the acquired ASSR, followed by the low-medium jitter and medium jitter. Thus, at 20 Hz in the central electrode, low jitter sequences better predict the response than medium jitter sequences, although less accurately than in the temporal electrode.

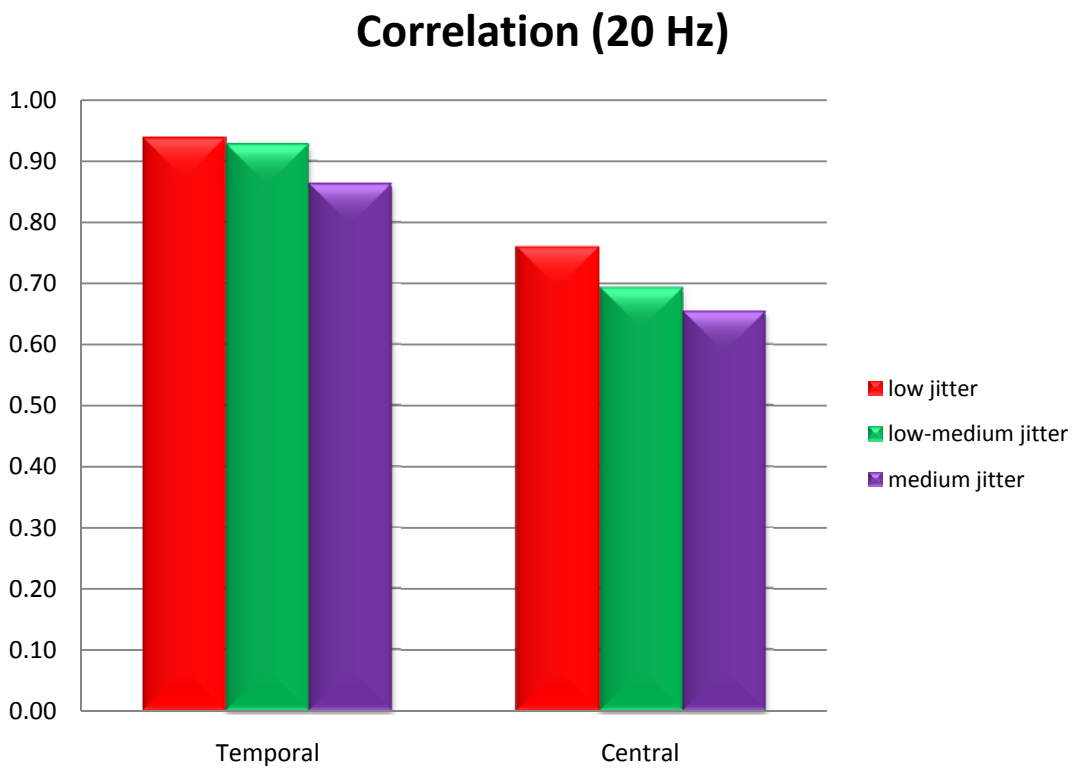

Figure 4.6. Mean correlation coefficient for four guinea pigs (Session # 8,10, 12, 13) at 20 Hz between the acquired and synthetic ASSRs for three sequences in temporal and central electrodes.

Comparison at 80 Hz rate

Due to the limited amount of data (1 animal, 2 Sessions) at 80 Hz, the comparison was only done for two sequences. As shown in **Figure 4.7**, in the temporal electrode, both sequences showed a fairly good prediction of the acquired ASSR, with a correlation coefficient typically above 0.7. As in all the cases reviewed, low jitter is the optimal sequence to predict the acquired ASSRs. The correlation coefficients for the central electrode were above 0.75, with low and low-medium jitter sequences equally predicting the acquired ASSR.

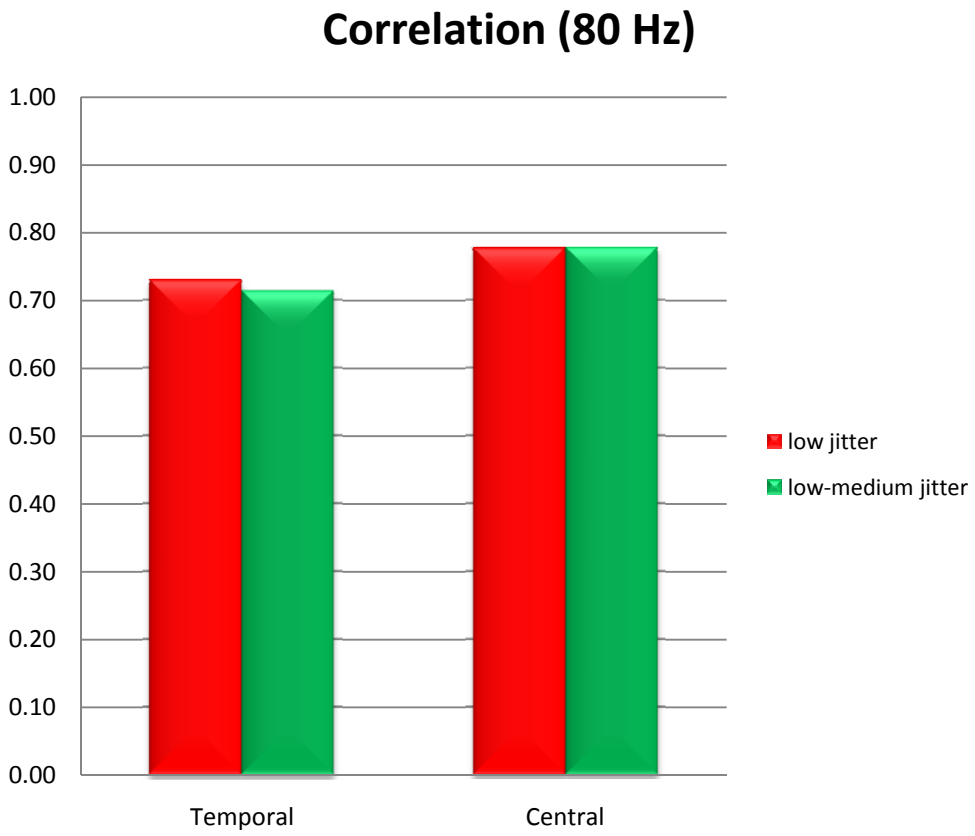

Figure 4.7. Mean correlation coefficient for one guinea pig (Session # 13) at 80 Hz between the acquired and synthetic ASSRs for two sequences in the temporal and central electrodes.

In terms of shape comparison provided by the correlation coefficient, it appears that at 20, 40, and 80 Hz, the transient responses were all able to predict the acquired ASSRs fairly accurately. The results improve with lower jittered sequences as compared to medium jittered sequences. In general, low jitter is best, followed by low-medium jitter and medium jitter.

4.2.2 Phasor Analysis

Phasor analysis was the final method used to compare the acquired and synthetic ASSRs. This study was done on the three main harmonics of the 20, 40, and 80 Hz responses.

Comparison at 40 Hz rate

In **Figure 4.8**, mean magnitudes of the acquired and synthetic 40 Hz ASSRs at its three main harmonics (40,80,120 Hz) are compared for the temporal electrode. The magnitude of the first harmonic (40 Hz) of the acquired data matches well to the respective low and low-medium jitter synthetic magnitudes. The synthetic data for the medium jitter, however, produced a lower magnitude. This is expected since medium-jitter creates different adaptation between varying intervals, thus smearing the synthetic data. The second and third harmonic magnitudes of the acquired and synthetic shows that the low and low-medium jitter sequences overestimate the acquired magnitude, while the medium jitter underestimates it. However, since most of the 40 Hz ASSRs' energy is found within its first harmonic, the variations in its other harmonics are negligible.

The same data is displayed in phasor form in **Figure 4.9.** It is clear that in all three harmonics, all the sequences share very similar phases, particularly in the first harmonic.

Therefore, as shown in both magnitude and phasor plots, the 40Hz ASSRs are best predicted by MLR recordings made by low and low-medium sequences, as opposed to medium jitter sequences. These results are verified in **Figure 4.10**, which displays the mean prediction errors plotted on a y-axis scale totaling the RMS signal magnitude. The

low jitter sequences clearly generate the least error in all three harmonics, followed by low-medium jitter and medium jitter.

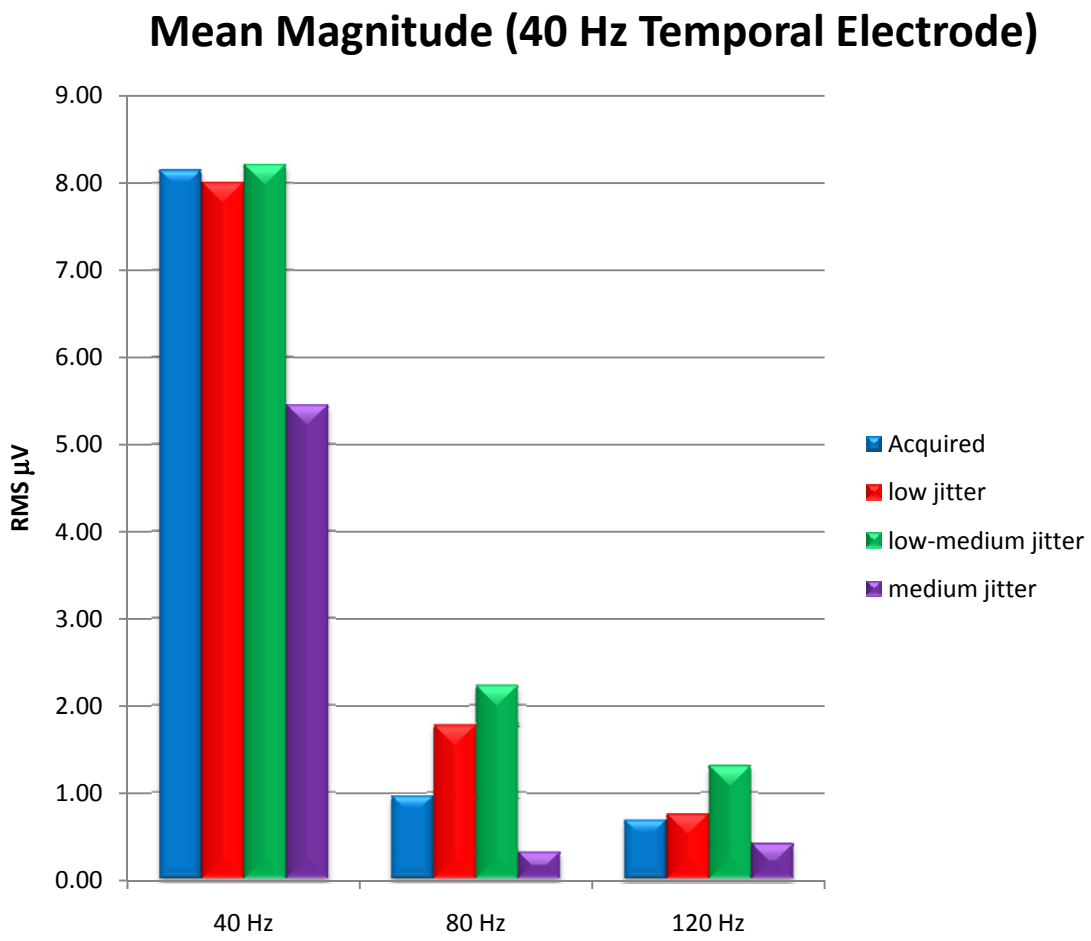

Figure 4.8. Mean magnitude comparison at the three main harmonic frequencies for five guinea pigs (Session # 10,12, 13, 25,26) at 40 Hz in the temporal electrode with three difference sequences.

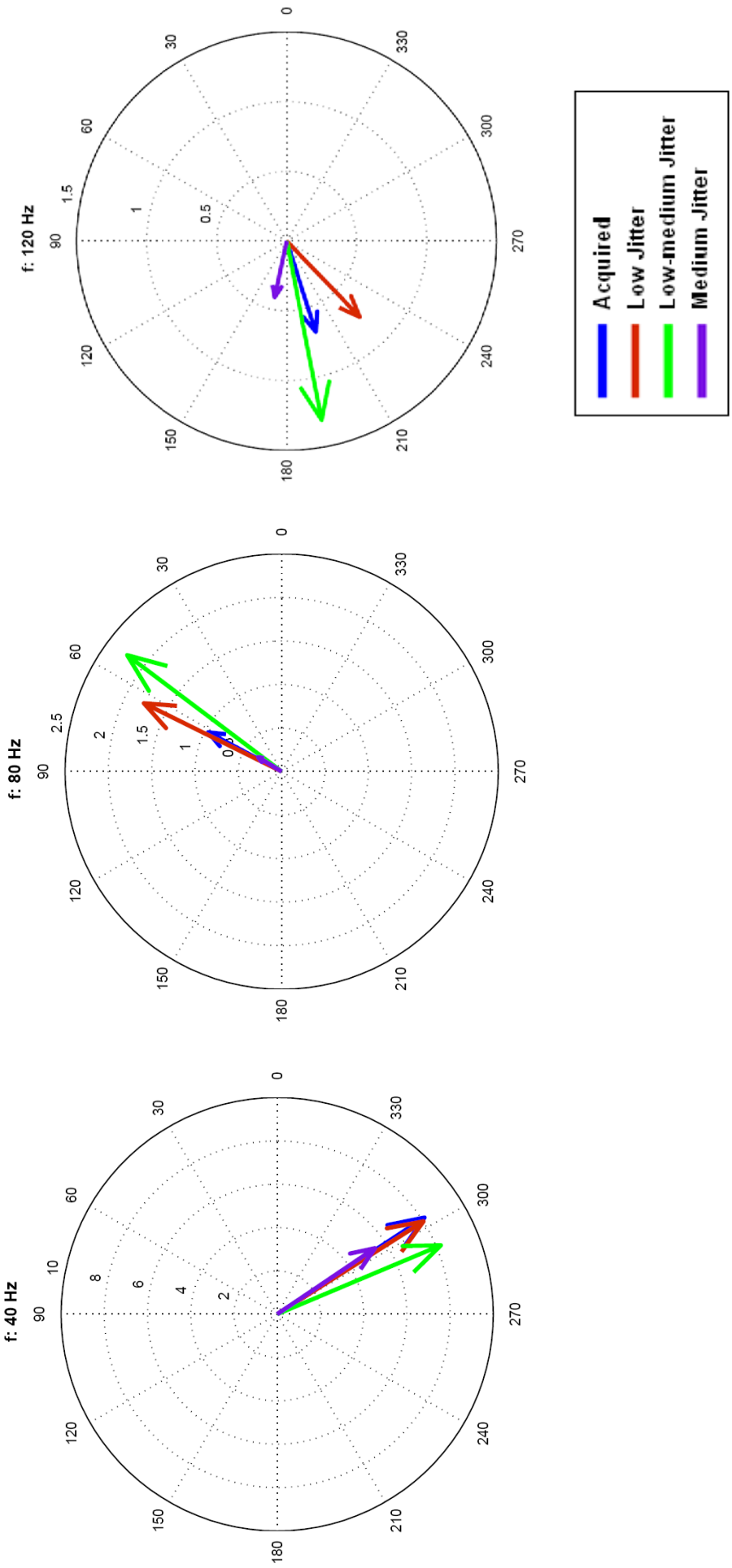

Figure 4.9. Mean vectorial averages at the three main harmonic frequencies for five guinea pigs (Session # 10,12, 13, 25,26) at 40 Hz in the temporal electrode with three difference sequences.

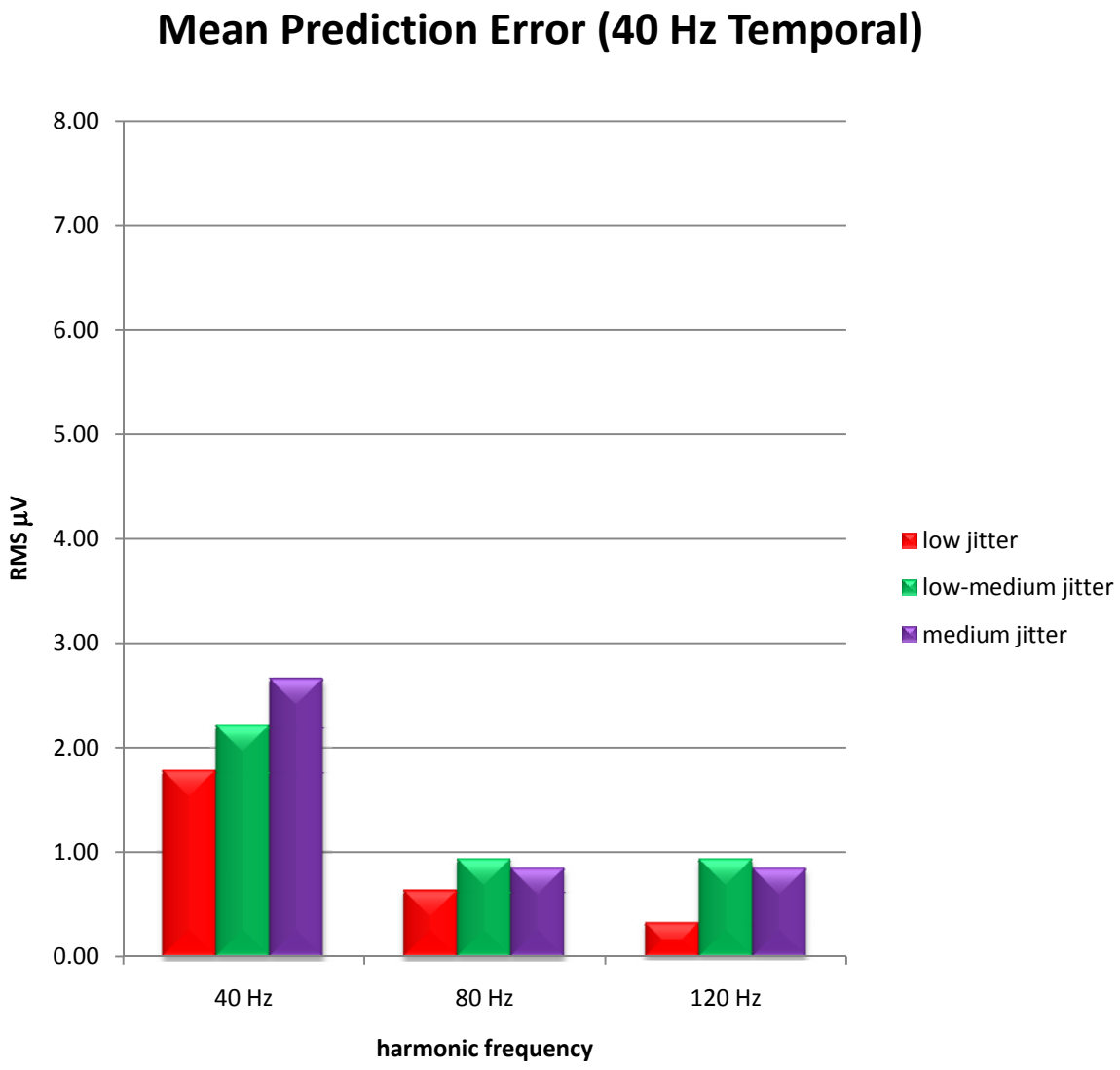

Figure 4.10. Mean prediction error of the mean magnitude at 40 Hz in the temporal electrode for its three main harmonic frequencies in five guinea pigs (Session # 10,12,13,25,26) with three different sequences. Mean prediction error is obtained by averaging the magnitude of the individual differences between the acquired and synthetic ASSRs.

The synthesized 40 Hz ASSR in the central electrode were also compared to the acquired ASSRs as shown in **Figure 4.11** and **4.12**. The mean magnitude plot shows that low-medium jitter sequences generate the magnitude that best predicts the acquired ASSR magnitude. Low jitter sequences and medium jitter sequences produce a lower magnitude. The magnitude appears to be best predicted by low-medium jitter, followed by low jitter and medium jitter. The phasor plots in **Figure 4.12** shows that all three sequences predict the acquired phase very accurately at all three main harmonics. The main harmonic (40 Hz) phase is best predicted by low and low-medium jitter sequences than medium jitter sequences. Finally, the mean prediction error results displayed in **Figure 4.13** shows the least error for low-jitter sequences, followed by low-medium jitter and medium-jitter sequences.

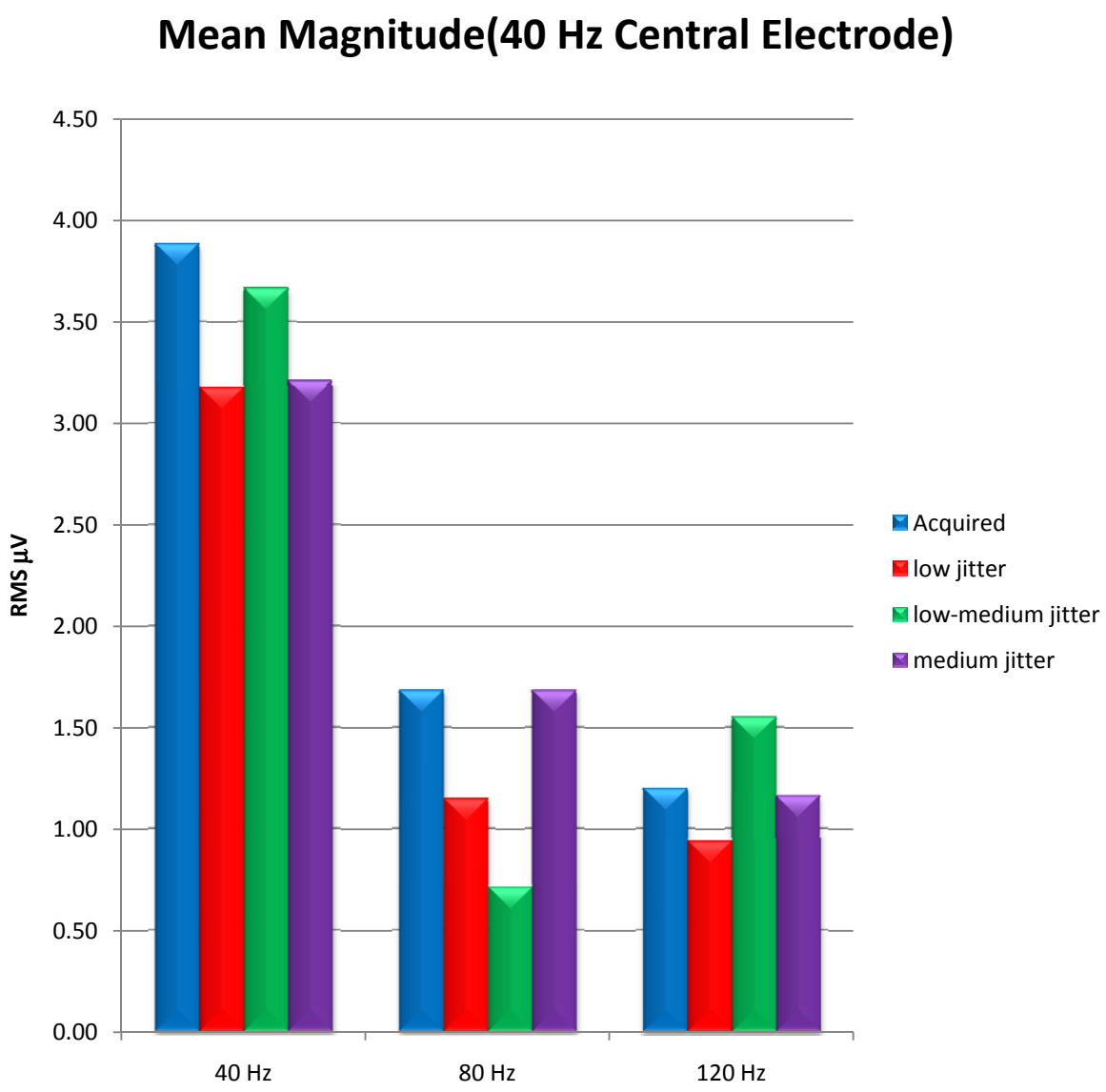

Figure 4.11. Mean magnitude comparison at the three main harmonic frequencies for five guinea pigs (Session # 10,12, 13, 25,26) at 40 Hz in the central electrode with three difference sequences.

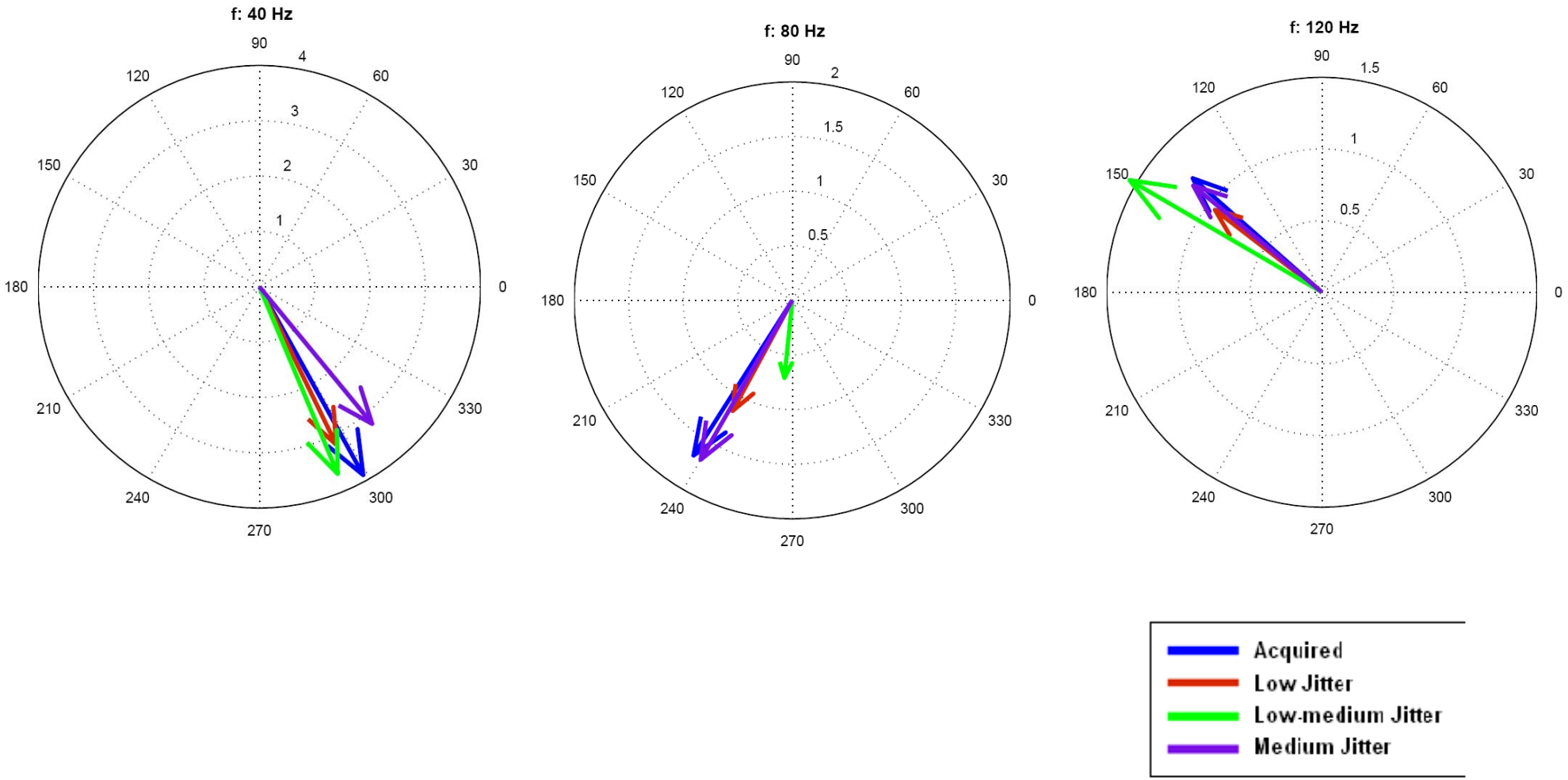

Figure 4.12. Mean vectorial averages at the three main harmonic frequencies for five guinea pigs (Session # 10,12, 13, 25,26) at 40 Hz in the central electrode with three difference sequences.

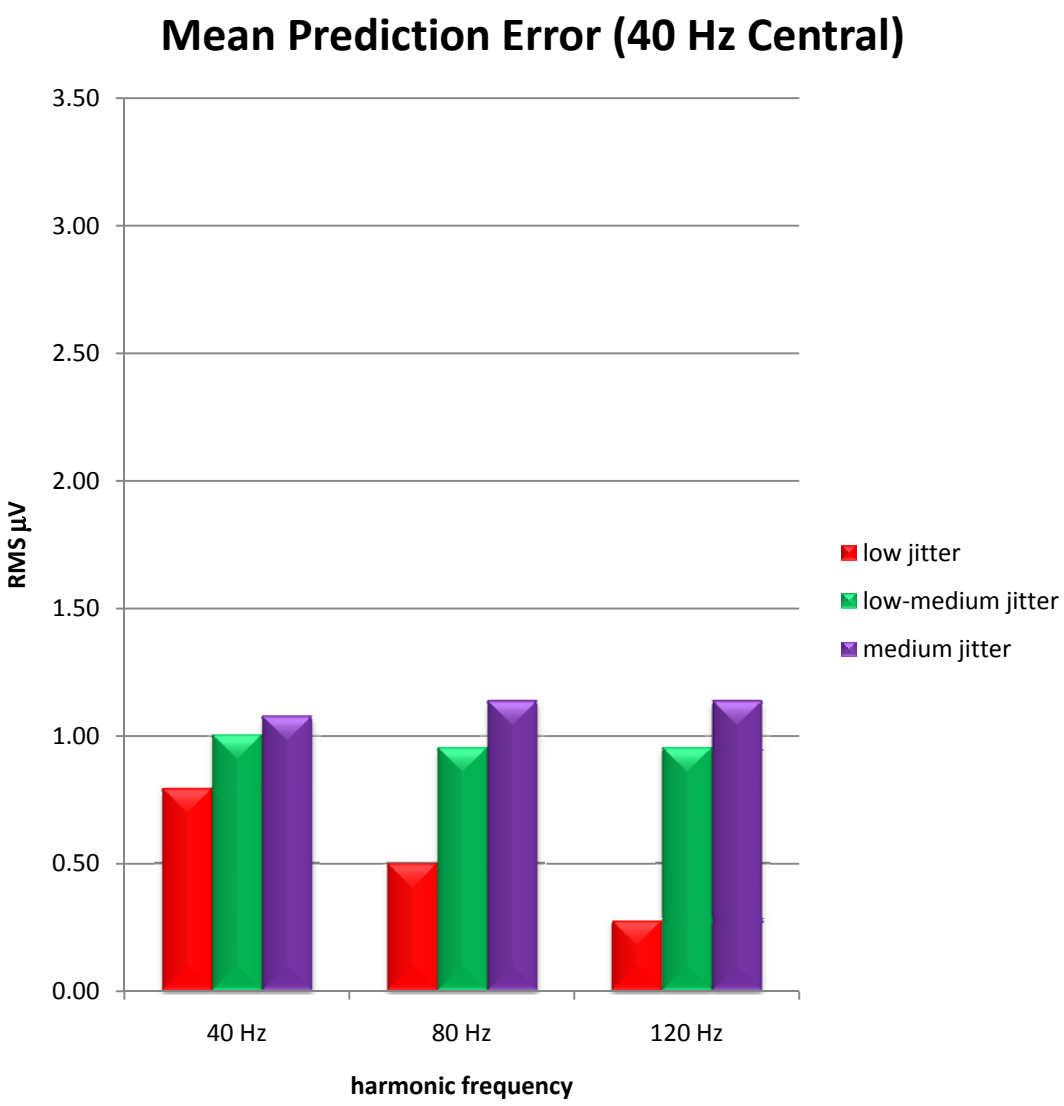

Figure 4.13. Mean prediction error of the mean magnitude at 40 Hz in the central electrode for its three main harmonic frequencies in five guinea pigs (Session # 10,12,13,25,26) with three different sequences. Mean prediction error is obtained by averaging the magnitude of the individual differences between the acquired and synthetic ASSRs.

Comparison at 20 Hz rate

Figure 4.14 shows the mean magnitudes of the acquired and synthetic 20 Hz ASSRs at its three main harmonics for the temporal electrode. In the main harmonics, all three sequences significantly overestimate the acquired ASSR magnitude. In the second and third harmonic, the low and low-medium jitter sequences overestimate the magnitudes and the medium-jitter underestimates it.

The phasor plots in **Figure 4.15** show an accurate prediction of the acquired phases for all three sequences at all three harmonics. In **Figure 4.16**, the mean prediction error shows that at the main harmonic, low jitter shows the least error, followed by low-medium jitter and medium jitter.

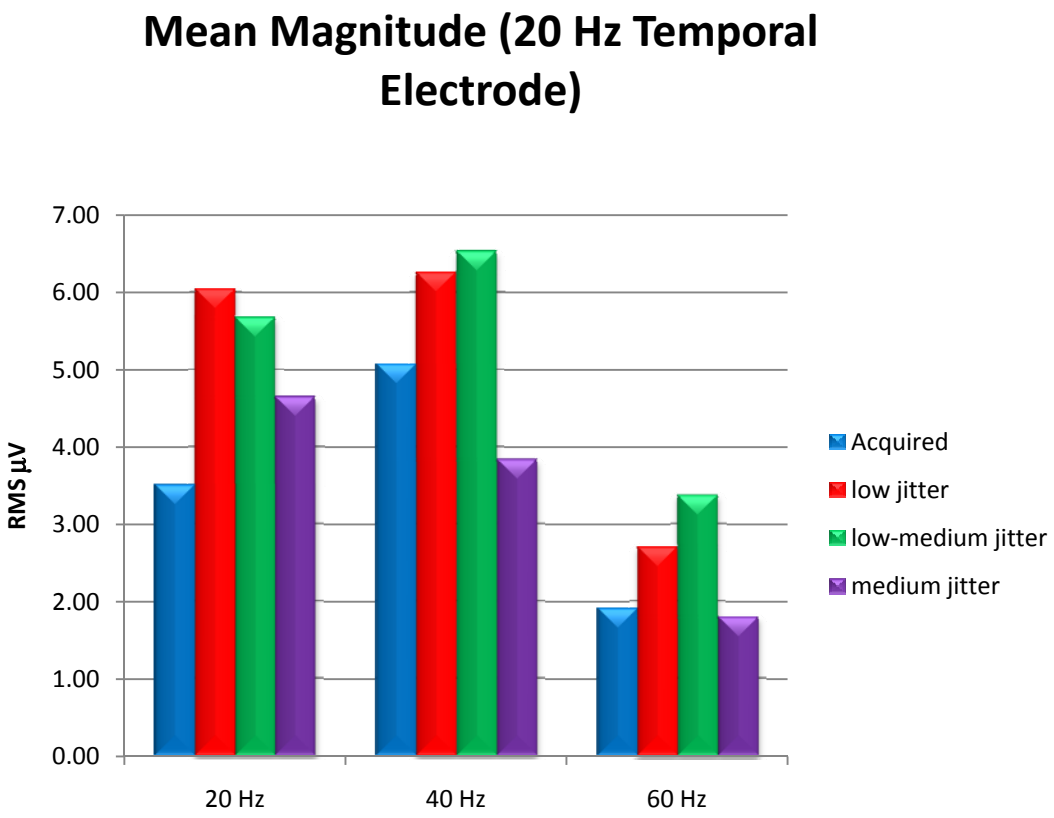

Figure 4.14. Mean magnitude comparison at the three main harmonic frequencies for four guinea pigs (Session # 8,10,12,13) at 20 Hz in the temporal electrode with three difference sequences.

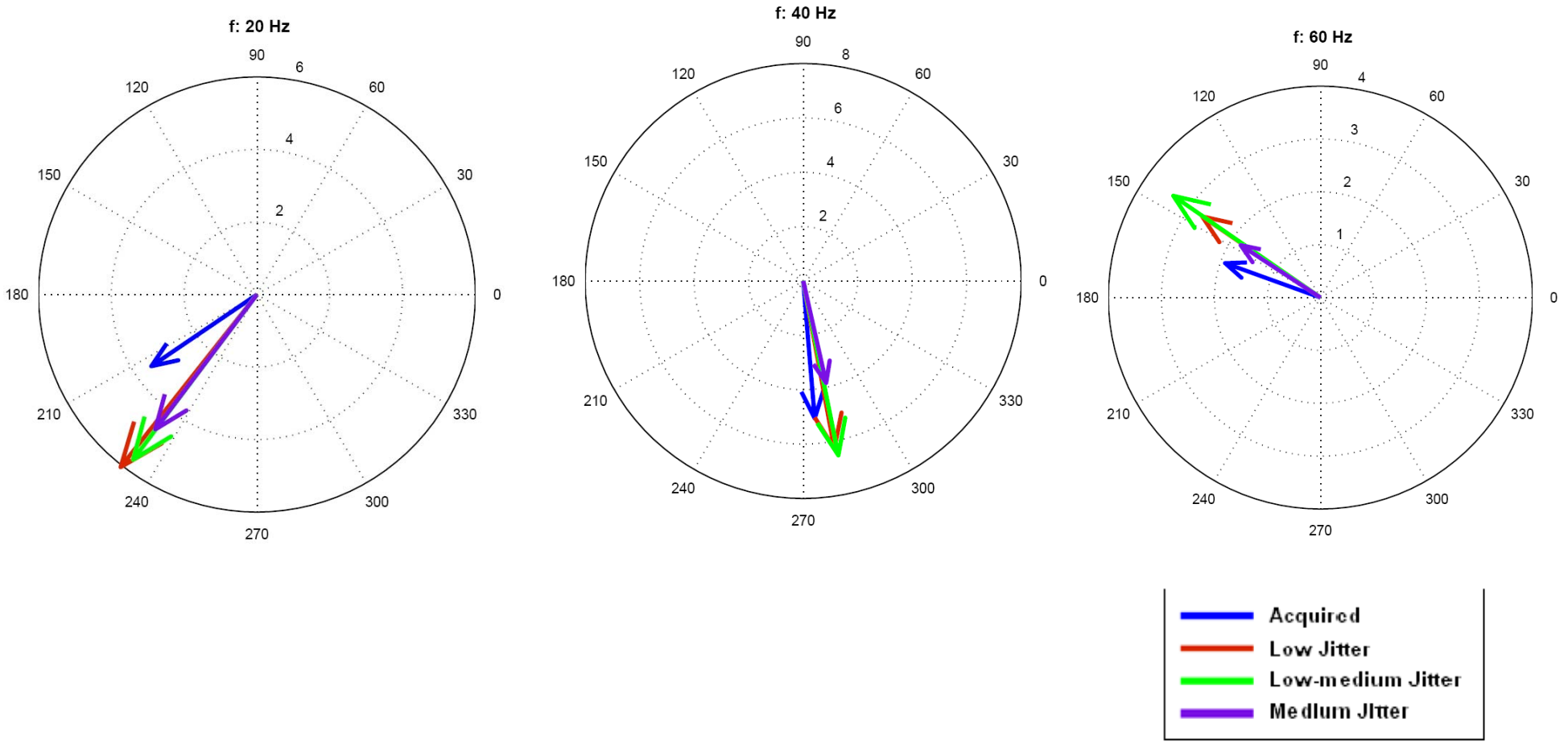

Figure 4.15. Mean vectorial averages at the three main harmonic frequencies for four guinea pigs (Session # 8,10,12,13) at 20 Hz in the temporal electrode with three difference sequences.

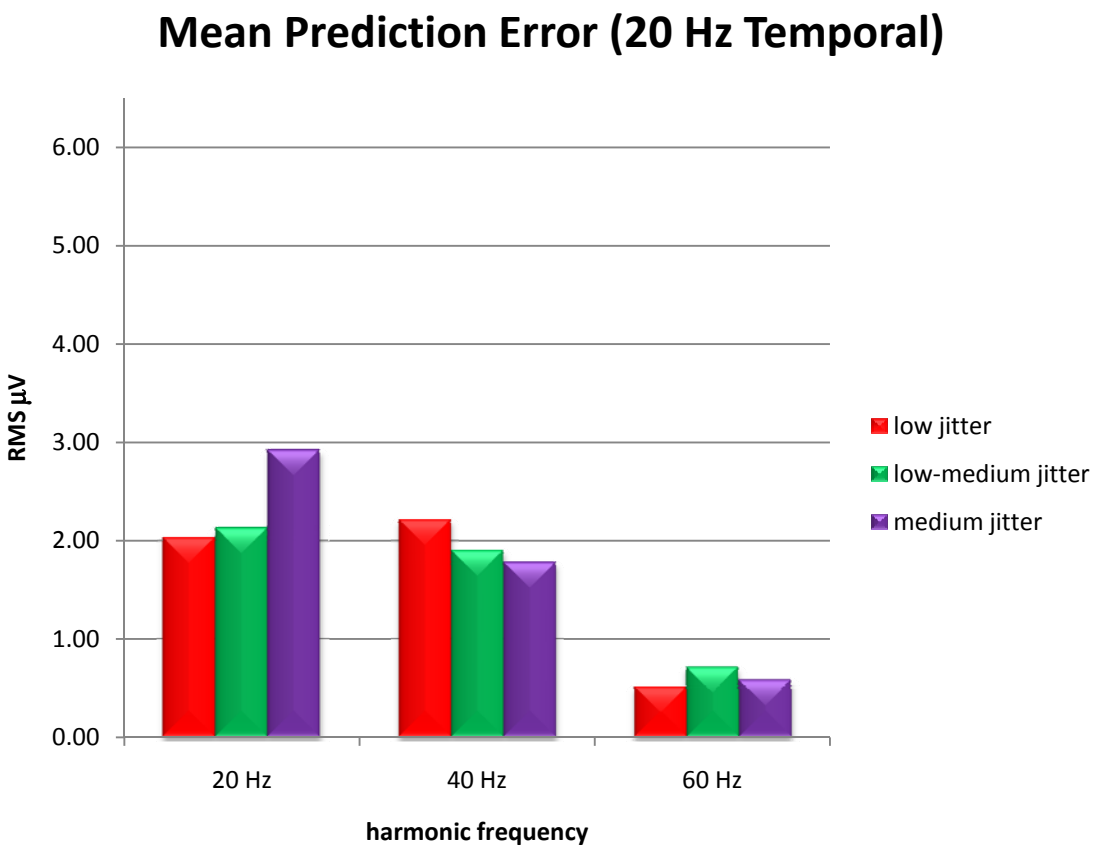

Figure 4.16. Mean prediction error of the mean magnitude at 20 Hz in the temporal electrode for its three main harmonic frequencies in four guinea pigs (Session # 8,10,12,13) with three different sequences. Mean prediction error is obtained by averaging the magnitude of the individual differences between the acquired and synthetic ASSRs.

Figure 4.17 shows the mean magnitude results for the 20 Hz central electrode. The main harmonic magnitude is overestimated by all three sequences. The phasor representation shown in **Figure 4.18** shows that at the main harmonic, all three sequences predict the phase accurately, with low and low-medium jitter being the closest. In **Figure 4.19**, the mean prediction error is shown to be least in the low jitter, followed by low-medium jitter and medium jitter. As emphasized earlier, the main harmonic is given the most emphasis since it holds the most energy in the signal's power spectrum.

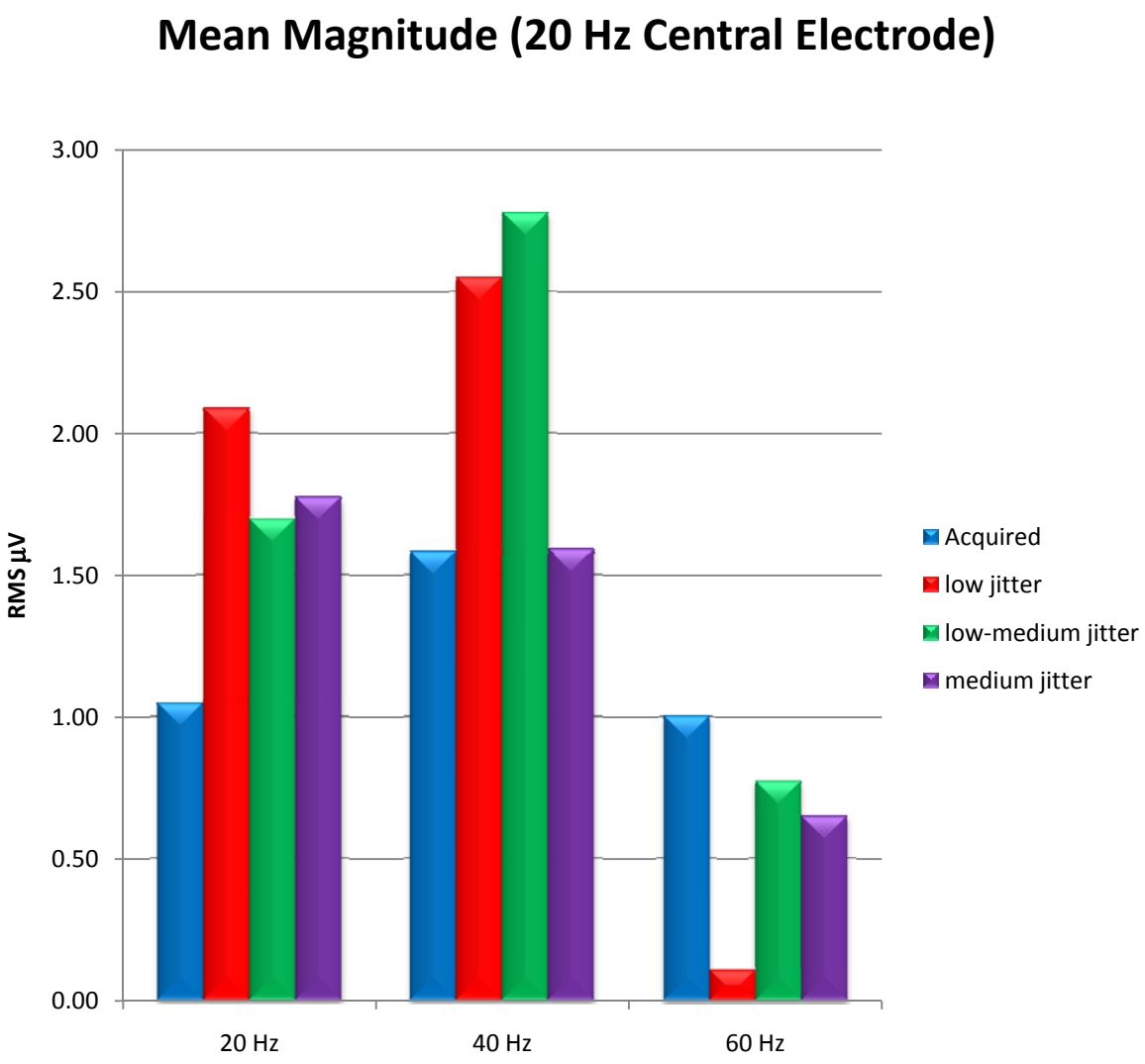

Figure 4.17. Mean magnitude comparison at the three main harmonic frequencies for four guinea pigs (Session # 8,10,12,13) at 20 Hz in the central electrode with three difference sequences.

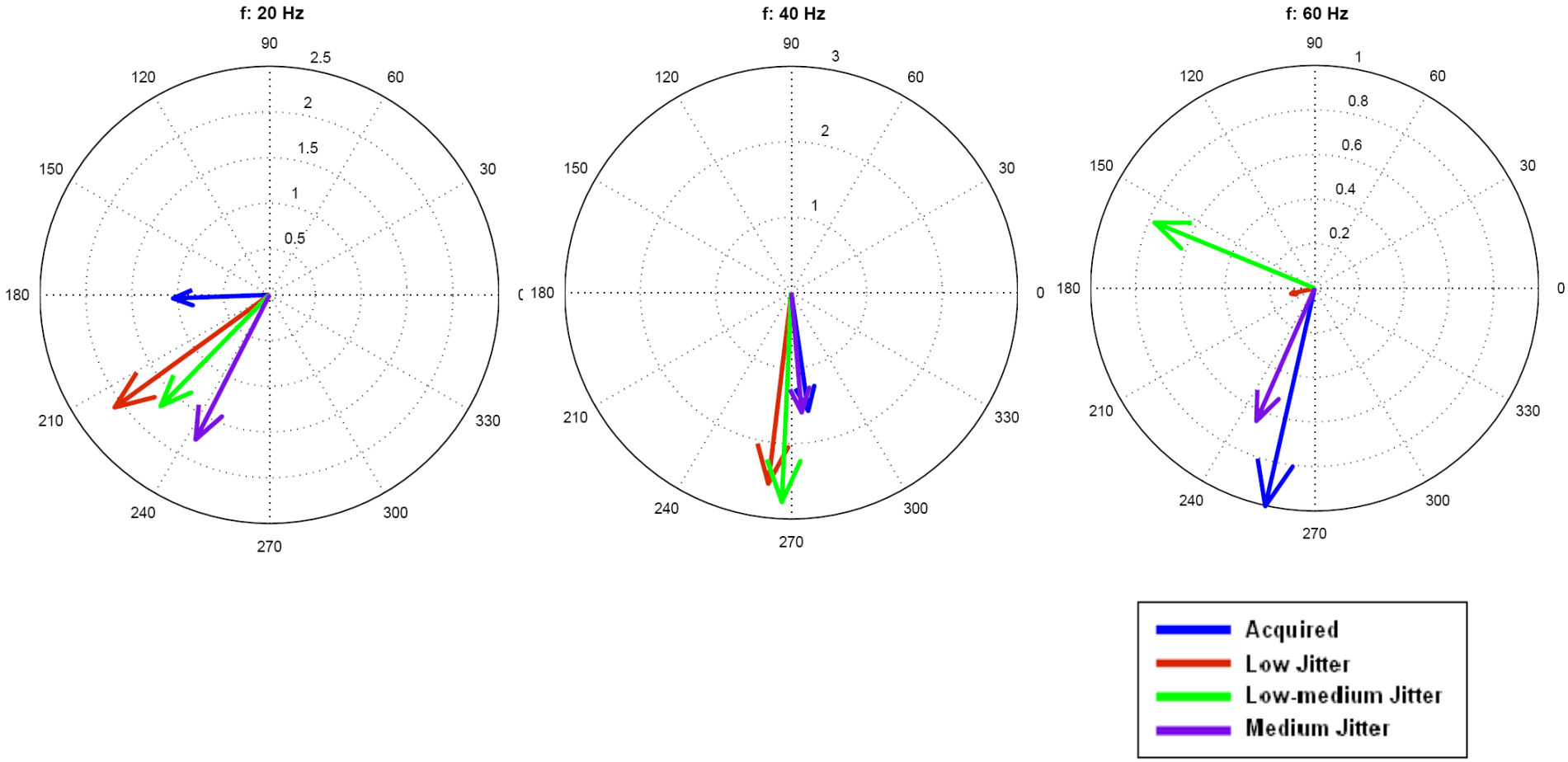

Figure 4.18. Mean vectorial averages at the three main harmonic frequencies for four guinea pigs (Session # 8,10,12,13) at 20 Hz in the central electrode with three difference sequences.

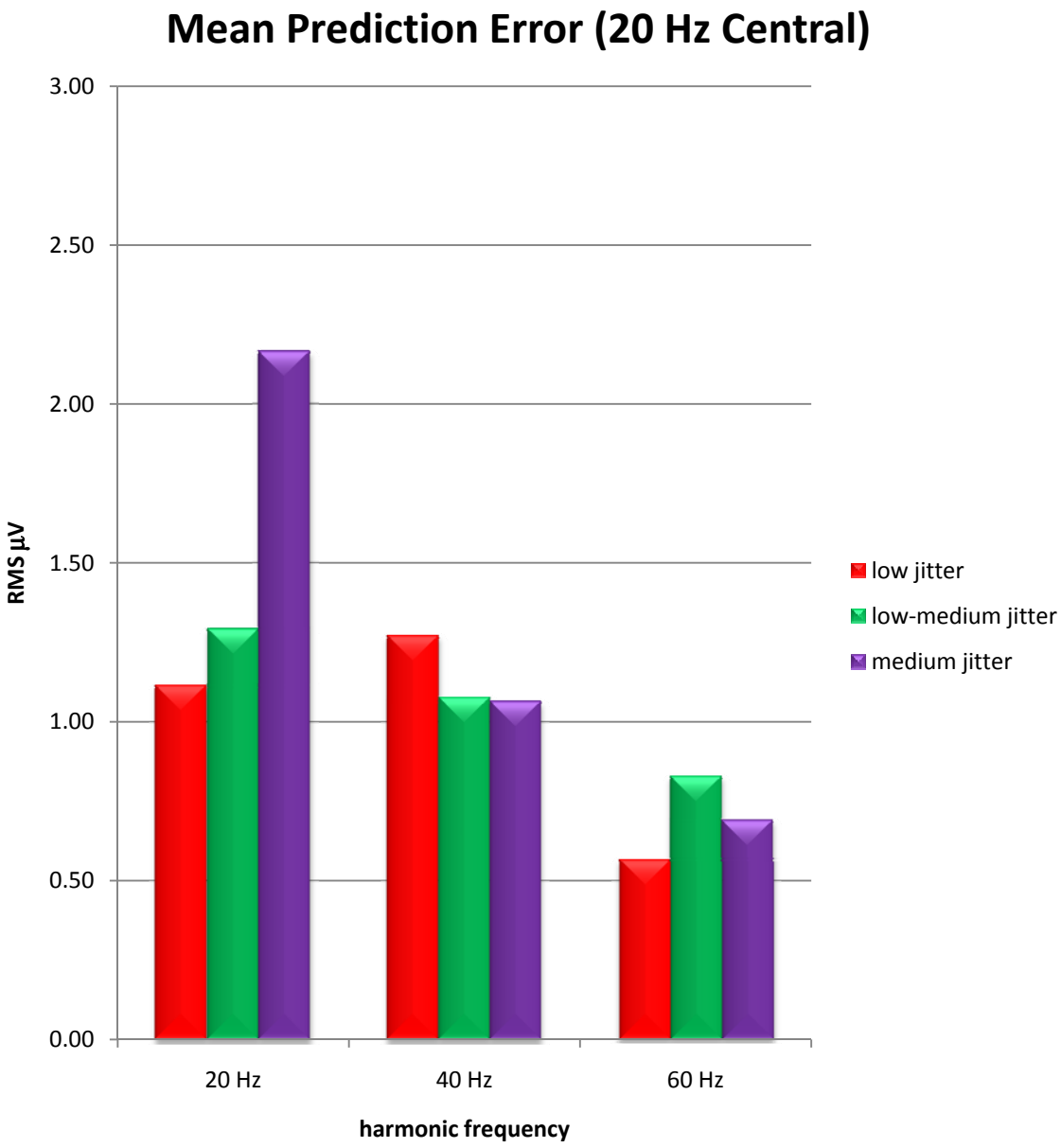

Figure 4.19. Mean prediction error of the mean magnitude at 20 Hz in the central electrode for its three main harmonic frequencies in five guinea pigs (Session # 8,10,12,13) with three different sequences. Mean prediction error is obtained by averaging the magnitude of the individual differences between the acquired and synthetic ASSRs.

Comparison at 80 Hz rate

Since the phasor comparison at 80 Hz was performed on only one animal, the following results presented should be taken with caution. As shown in **Figure 4.20**, in the temporal electrode, the mean magnitude of the acquired ASSR was significantly overestimated for both low and low-medium jitter sequences in the main harmonic. Despite the magnitude differences, the phasor analysis in **Figure 4.21** shows that the phases were very accurately predicted, especially in the main harmonic. The mean prediction error was not calculated for 80 Hz due to the limited amount of data.

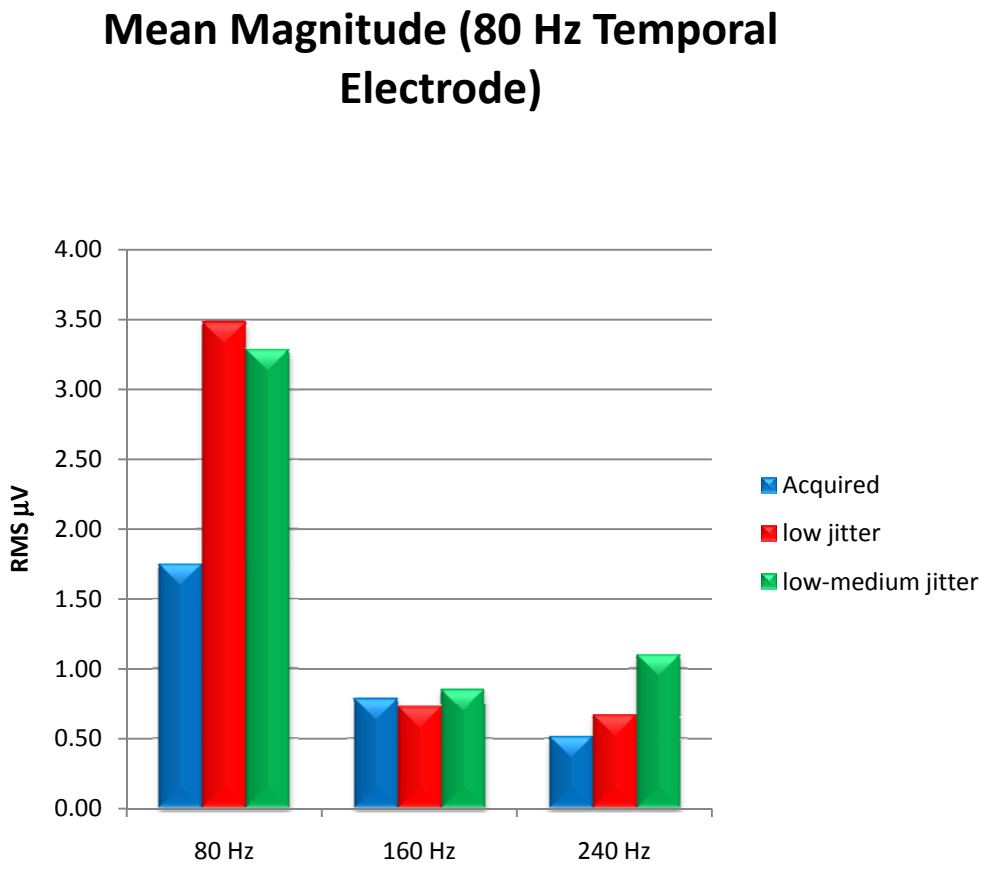

Figure 4.20. Mean magnitude comparison at the three main harmonic frequencies for one guinea pig (Session # 13) at 80 Hz in the temporal electrode with three difference sequences.

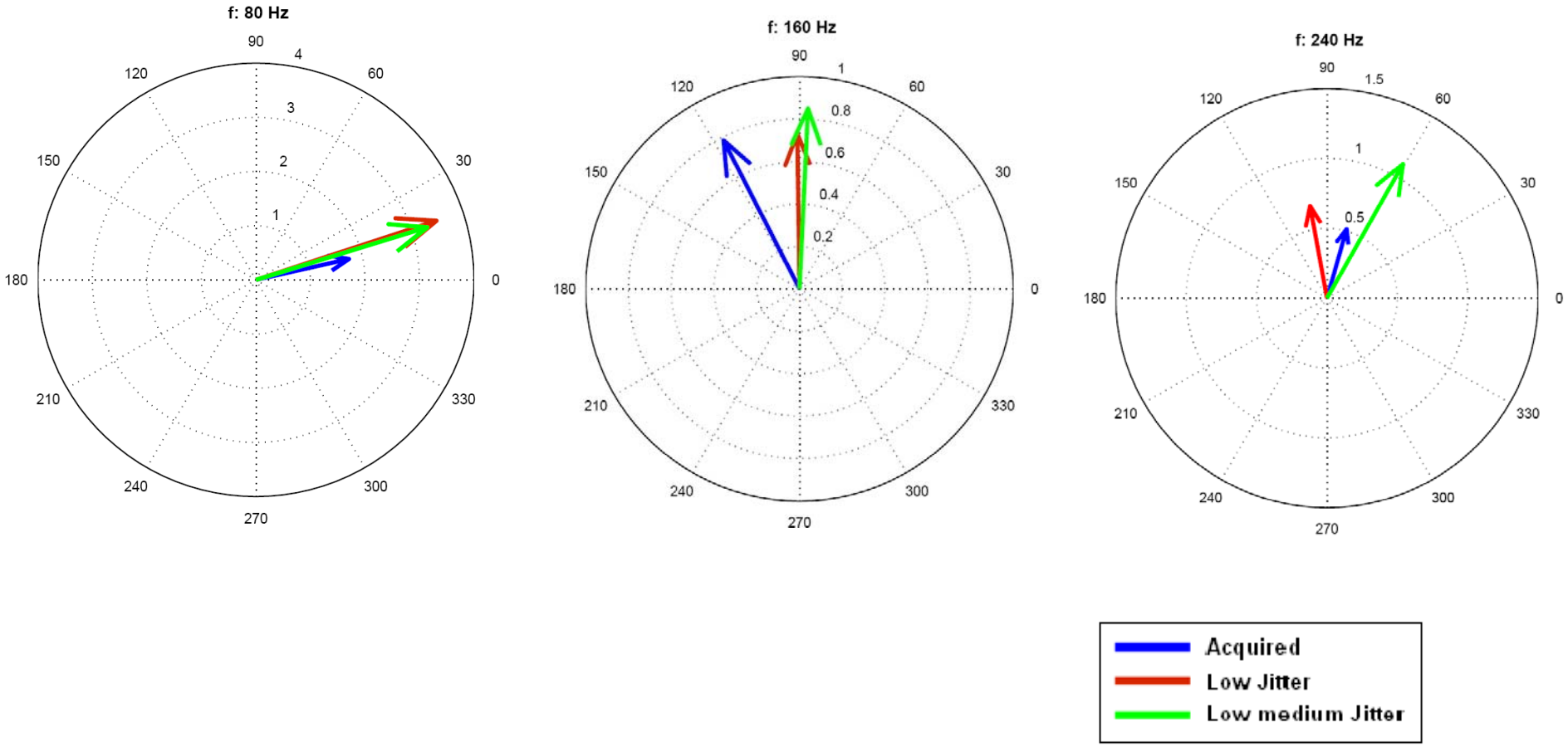

Figure 4.21. Mean vectorial averages at the three main harmonic frequencies for one guinea pig (Session # 13) at 80 Hz in the temporal electrode with three difference sequences.

The results for the 80 Hz central electrode are shown in **Figure 4.22** and **Figure 4.23**. As in the temporal electrode, the mean magnitudes are over predicted for both low and low-medium sequences, although to a lesser degree. The phasor analysis shows a very good prediction of the acquired ASSR phases, with low-medium jitter generating the best phase prediction.

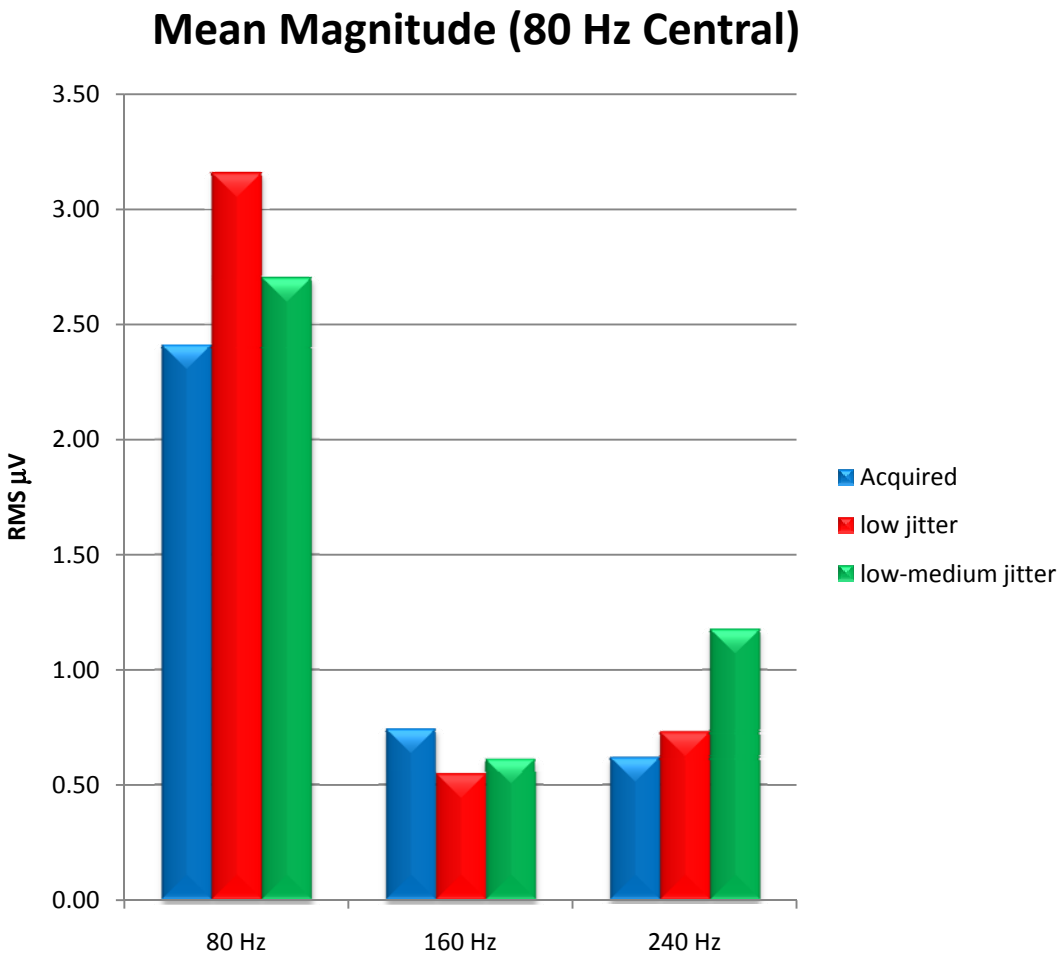

Figure 4.22. Mean magnitude comparison at the three main harmonic frequencies for one guinea pig (Session # 13) at 80 Hz in the central electrode with three difference sequences.

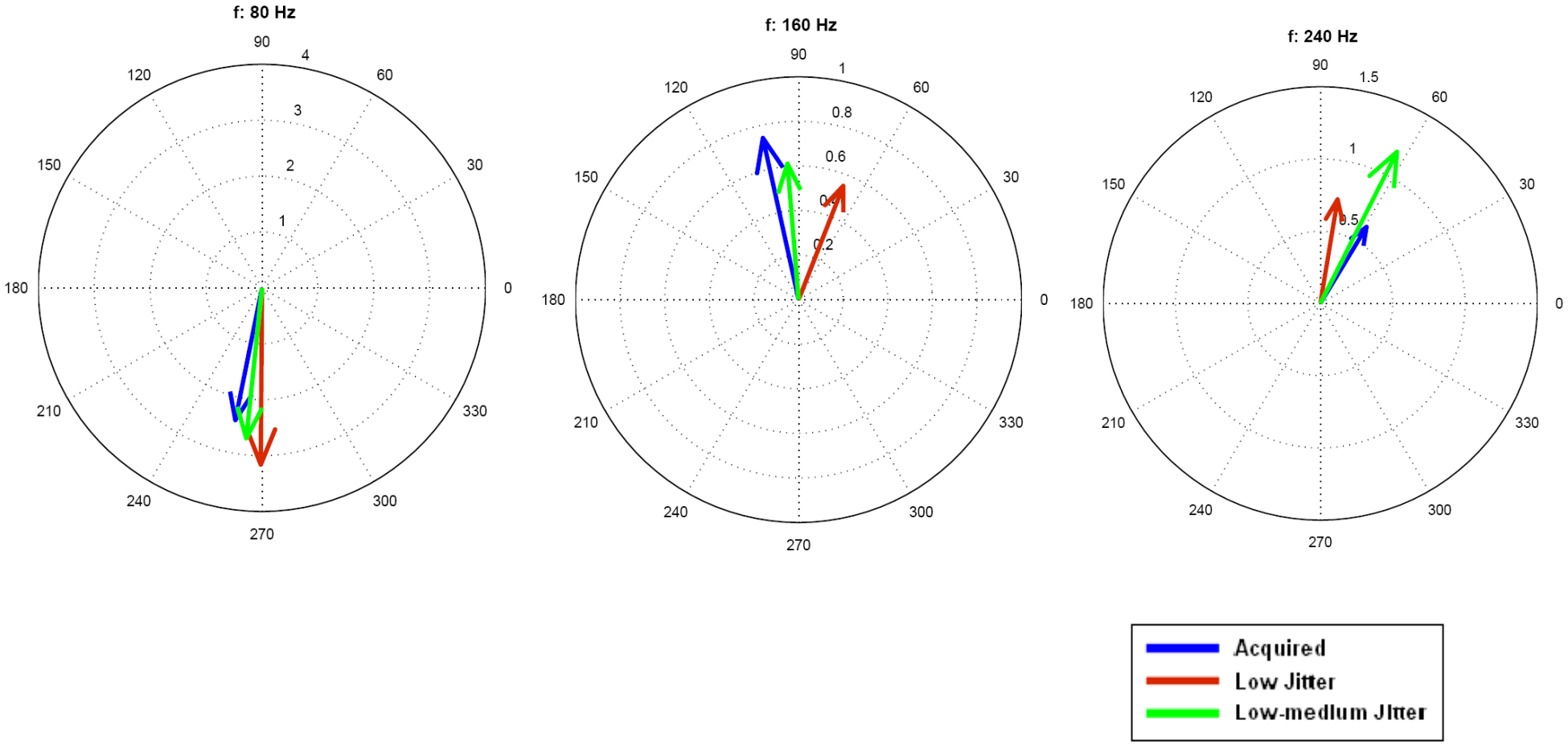

Figure 4.23. Mean vectorial averages at the three main harmonic frequencies for one guinea pig (Session # 13) at 80 Hz in the central electrode with three difference sequences.

Overall, in recordings at 40 Hz (temporal electrode), the superposition of the MLR responses does explain the generation of the 40 Hz ASSR as demonstrated by both magnitude and phase analysis. The recordings made in the central electrode predict the acquired ASSR in its phases, but there are some magnitude differences. Similarly, at 20 and 80 Hz in both temporal and central electrodes, the synthetic ASSRs did not appear to fully predict the acquired ASSRs. Although the phases were closely predicted, large magnitude variations were common.

4.3 Further Discussions

Recent studies have shown that various endogenous events can affect the acquired ASSRs. The main factors include: sleep and mental state (Galambos et al., 1981; Stapells et al., 1984; Hori et al., 1993). In addition, time of recordings, trivial noise in the recordings, and insert ear phone positioning could have affected the recorded response.

Even in the absence of muscle tension that affects a signal, worrying, excitement, and other mental states can alter AERs. The major lesson from this study is to understand that EEG data should always be recorded in order to analyze responses, which are affected by a subject's mental state. Since the guinea pig EEG data used in this study were not recorded, it is impossible to determine the impact that mental state had on the results. Analyzing the various parameters in the study revealed that the time between recordings fluctuated, providing an opportunity for the animal to undergo changes in mental state. Therefore, it is best to keep time between recordings to a minimum in an attempt to prevent the onset of a change in mental state. A review of the analyzed data, however, did not appear to show any significant changes as time between recordings fluctuated.

Finally, another source of error skewing the results is the additive noise generated from phase locking. Due to the time-shifted cyclical continuous loop summation property in convolution, minor noise in the recordings is phase-locked, creating a significant source of noise in the final computed ASSR.

CHAPTER 5: CONCLUSION

This research involved studying two major phenomena in the guinea pig auditory evoked responses using data collected over the summer of 2007 in Ankara, Turkey. The first part of this study aimed at investigating the ASSR resonance characteristics as a function of rate in guinea pigs. A study of the grand average of the mean amplitudes of all the guinea pigs revealed a resonance around 40 Hz. This finding is shared in humans at 40 Hz (Galambos et al., 1981), rats (Conti et al., 1999) at 50 Hz, and rabbits (Ottovani, et al., 1990) and cats (Makela et al., 1990) at 30 Hz. However, unlike the human 40 Hz ASSR, the guinea pig ASSR resonance is very broad (26-52 Hz) and flat. The centrally recorded ASSRs are smaller and tend to have resonances at higher rates compared to temporal signals.

The second part of the analysis investigated the superposition theory in predicting the acquired ASSRs at each corresponding rate. This theory is one of two competing theories on the origin of the ASSRs, with the other centering on the induced phase synchronization of brain waves. In order to test the superposition theory, transient responses were used to create synthetic ASSRs, which were then compared to the acquired ASSRs via correlation coefficient and phasor analysis. For the 40 Hz ASSR, both temporal and central electrode synthesized ASSRs show a correlation coefficient above 0.80. At 20 Hz ASSRs, the correlation coefficient is very high (~0.9) in the temporal electrode, yet significantly lower (~0.7) for the central electrode. Finally, at 80 Hz, the correlation coefficient is significantly lower in both temporal and central electrodes (~0.7). At all rates, the correlation coefficients are highest with low jitter sequences.

Finally, phasor analysis was also used to test the superposition theory of the generation of the acquired ASSRs at 20,40, and 80 Hz. Overall, in the recordings at 40 Hz (temporal electrode), the superposition of the MLR responses accurately predicts the acquired 40 Hz ASSR as demonstrated by both magnitude and phase analysis. The recordings made in the central electrode only predicted the acquired ASSR in its phases, with significant differences found in magnitude at its main harmonics. Similarly, at 20 and 80 Hz in both temporal and central electrodes, the synthetic ASSRs did not appear to fully predict the acquired ASSRs. Although the phases were successfully predicted, large magnitude variations were observed. As shown by mean prediction error plots, phasor analysis shows that the acquired ASSR is best predicted with low jitter sequences, followed by low-medium and medium jitter sequences.

It is important to note that the acquired ASSR data utilized in this research could have been affected by the following: sleep, mental state, time between recordings, and insert ear phone positioning. This is significant, since these parameters were not monitored and a combination of these variables could have impacted the results. Future experiments should focus on improving testing environment conditions to minimize these sources of error.

REFERENCES

Aoyagi, M., Kiren, T., Kim, Y., Suzuki, Y., Fuse, T., & Koike, Y. (1993). Optimal modulation frequency for amplitude-modulation following response in young children during sleep. *Hearing Research* , 65:253-261.

Azzena, G., Conti, G., Santarelli, R., Ottaviani, F., Paludetti, G., & Maurizi, M. (1995). Generation of human auditory steady-state responses (SSRs). I: Stimulus rate effects. *Hearing Research* , 83:1-8.

Basar, E. (1980). *EEG-Brain Dynamics: Relation between EEG and Brain Evoked Potentials.* Amsterdam: Elsevier.

Basar, E., Rosen, B., Basar-Eroglu, C., & Greitschus, F. (1987). The associations between 40 Hz-EEG and the middle latency response of the auditory evoked potential. *International Journal of Neuroscience* , 33:103-117.

Bohórquez, J., & Özdamar, Ö. (2008). Generation of the 40 Hz auditory steady state response (ASSR) explained using convolution. *Clinical Neurophysiology* , Revision in submission.

Bressler, S. (1990). The gamma-wave: a cortical information carrier? *Trends in Neuroscience* , 13:161-162.

Buchwald, J., Hinman, C., Norman, R., Huang, C., & Brown, K. (1981). Middle and long-latency auditory evoked responses recorded from the vertex of normal and chronically-lesioned cats. *Brain Research* , 205:91-109.

Chiappa, KH. (1990). Brainstem auditory evoked potentials: methodology. In: KH. Chiappa (ed), *Evoked Potentials in Clinical Medicine (*pp 173–221). New York: Raven Press.

Cohen, L., Rickards, F., & Clark, G. (1991). A comparison of steady-state evoked potentials to modulated tones in awake and sleeping humans. *Journal of Acoustical Society of America* , 90:2467-2479.

Conti, G., Santarelli, R., Grassi, C., Ottaviani, F., & Azzena, G. (1999). Auditory steady-state responses to click trains from the rat temporal cortex. *Clinical Neurophysiology* , 110: 62-70.

Demirtas, S., Özdamar, Ö. (2008). Auditory cortical responses in guinea pigs as a function of stimulus rate. Personal communication.

Firsching, R., Luther, J., Eidelberg, E., Brown, W., Story, J., & Boop, F. (1987). A 40 Hz middle latency auditory evoked response in comatose patients. *Electroencephalography and Clinical Neurophysiology* , 67: 213-216.

Galambos, R. (1982). Tactile and auditory stimuli presented at high rates (30-50 per s) produce similar even related potentials. *Annals of New York Academy of Science* , 88:722-728.

Galambos, R., & Makeig, S. (1988). Dynamic changes in steady-state responses. In E. Basar, *Dynamics of Sensory and Cognitive Processing by the Brain* (pp. 103-122). Berlin: Springer.

Galambos, R., Makeig, S., & Talmachoff, P. (1981). A 40 Hz auditory potential recorded from the human scalp. *Proceedings of the National Academy of Sciences* , 78:2643-2647.

Goksoy, C., & Utkucal, R. (2000). Binaural interaction component and white-noise enhancement in middle latency responses: differential effects of anaesthesia in guinea pigs. *Exp. Brain Res.* , 130: 410-414.

Greenberg, RP., Newton, PG., Hyatt, MS., Narayan, RK. & Becker, DP. (1981). Prognostic implications of early multimodality evoked potentials in severely head injured patients. A prospective study. *Journal of Neurosurgery* , 55:227-236.

Hood, L., & Berlin, C. (1986). Auditory Evoked Potentials, Pro-Ed editors. Austin, Texas.

Hori, A., Yasuhara, A., Naito, H., & Yasuhara, M. (1993). Steady-state auditory evoked potentials (SSAEPs) in the rabbit. Contribution of the inferior colliculus. *Electroencephalography and Clinical Neurophysiology* , 88:229-236.

Jansen, B., Agarwal, G., Hegde, A., & Boutos, N. (2003). Phase synchronization of the ongoing EEG and auditory EP generation. *Clinical Neurophysiology* , 114:79-85.

Jerger, J., Frost, J., & Cocker, N. (1986). Effect of sleep on the auditory steady state potential. *Ear and Hearing* , 7:240-245.

Kiang, N., Neame, J., & Clark, L. (1961). Evoked electrical activity from auditory cortex in anesthetized and unanesthetized cats. *Science* , 133:1927.

Kraus, N., Özdamar, Ö., & Hier, D. (1982). Auditory middle latency responses (MLRs) in patients with cortical lesions. *Electroencephalography and Clinical Neurophysiology* , 54:275-287.

Kraus, N., Smith, D., & Mcgee, T. (1988). Midline and temporal lob MLRs in the guinea pig originate from different generator systems: A conceptual framework from new and existing data. *Electroencephalography and Clinical Neurophysiology* , 71: 541-558.

Levi, E., Folsom, R., & Dobie, R. (1993). Amplitude-modulation following response (AMFR): Effects of modulation rate, carrier frequency, age, and state. *Hearing Research* , 68:42-52.

Linden, R., Campbell, K., Hamel, G., & Picton, T. (1985). Human auditory steady state evoked potentials during sleep. *Ear and Hearing* , 6:167-174.

Lins, O., Picton, P., Picton, T., Champagne, S., & Durieux-Smith, A. (1995). Auditory steady-state responses to tones amplitude-modulated at 80-110 Hz. *Journal of Acoustical Society of America* , 97:3051-3063.

Lins, O., Picton, T., Boucher, B., Durieux-Smith, A., Champagne, S., Moran, L., et al. (1996). Frequency-specific audiometry using steady-state responses. *Ear and Hearing* , 17:81-96.

Mäkelä, J., Karmos, G., Molnar, M., Csepe, V., & Winkler, I. (1990). Steady-state responses from the cat auditory cortex. *Hearing Research* , 45:41-50.

McGee, T., Özdamar, Ö., & Kraus, N. (1983). Auditory Middle Latency Responses in the Guinea Pig. *American Journal of Otolaryngology* , 4:116-122.

Michelini, S., Arslan, E., Prosser, S., & McKean, C. (1982). Logarthmic display of auditory evoked potentials. *Journal of Biomedical Engineering* , 4:62-64.

Ottovani, F., Paludetti, G., Grassi, S., Draicchio, F., Santarelli, R., Serafini, G., et al. (1990). Auditory steady responses in the rabbit. *Audiology* , 29:212-218.

Özdamar, Ö., & Bohórquez, J. (2007). Pb(P1) resonance at 40 Hz: Effects of high stimulus rate on auditory middle latency responses (MLRs) explored using deconvolution. *Clinical Neurophysiology* , 118:1261-1273.

Özdamar, Ö., & Bohórquez, J. (2006). Signal to noise ratio and frequency analysis of continuous loop averaging deconvolution (CLAD) of overlapping evoked potentials. *The Journal of the Acoustical Society of America* , 119:429-438.

Özdamar, Ö., & Kraus, N. (1983). Auditory middle-latency responses in humans. *Audiology* , 22:34-49.

Özdamar, Ö., Kraus, N., & Curry, F. (1982). Auditory brainstem and middle latency responses in a patient with cortical deafness. *Electroencephalography and Clinical Neurophysiology* , 53:224-230.

Patterson, J., Owen, C., Silberstein, R., Simpson, D., Nield, G., & Pipingas, A. (1998). SSVEP changes in response to olfactory stimulation. *Annals of New York Academy of Sciences* , 855:625-627.

Picton, T., John, M., Dimitrijevic, A., & Purcell, D. (2003). Human auditory steady-state responses. *International Journal of Audiology* , 42:177-219.

Plourde, G., & Picton, T. (1990). Human auditory steady-state response during general anesthesia. *Anesthesia & Analgesia* , 71:460-468.

Regan, D. (1989). *Human Brain Electrophysiology: Evoked Potentials and Evoked Magnetic Fields in Science and Medicine.* Amsterdam: Elsevier.

Rickards, F., Tan, L., Cohen, L., Wilson, O., Drew, J., & Clark, G. (1994). Auditory steady-state evoked potential in newborns. *British Society of Audiology* , 28:327-337.

Robinson, K. & Rudge, P. (1977). Abnormalities of the auditory evoked potentials in patients with multiple sclerosis. *Brain* , 100:19-40.

Rössner, W. (1965). *Stereotaktisher Hirnatlas vom Meerschweinchen.* Munich: Palla Velag.

Santarelli, R., Maurizi, M., Conti, G., Ottaviani, F., Paludetti, G., & Pettorossi, V. (1995). Generation of human auditory steady-state responses (SSRs). II: Addition of responses to individual stimuli. *Hearing Research* , 83:9-18.

Sayers, B., Beagley, H., & Henshall, W. (1974). The mechanism of auditory evoked EEG responses. *Nature* , 247:481-483.

Spydell, J., Pattee, G., & Goldie, W. (1985). The 40 Hz auditory event-related potential: normal values and effects of lesions. *Electroencephalography and Clinical Neurophysiology* , 62: 193-202.

Stapells, D., Galambos, R., Costello, J., & Makeig, S. (1988). Inconsistency of auditory middle latency and steady-state responses in infants. *Electroencephalography and Clinical Neurophysiology* , 71:289-295.

Stapells, D., Linden, D., Suffield, J., Hamel, G., & Picton, T. (1984). Human auditory steady state potentials. *Ear & Hearing* , 5:105-113.

Teas, D., & Kiang, N. (1964). Evoked responses from the auditory cortex. *Exp Neurol* , 10:91-119.

Yoshida, M., Lowry, L., Liu, J., & Kaga, K. (1984). Auditory 40 Hz responses in the guinea pig. *American Journal of Otolaryngology* , 5: 404-410.